

Matija Cuzovic

Analysis of the Fatigue Behavior of 3D-Printed Maraging 300 Steel

Master's thesis in Produktutvikling og produksjon

Supervisor: Filippo Berto

June 2020

NTNU
Norwegian University of Science and Technology
Faculty of Engineering
Department of Mechanical and Industrial Engineering

Matija Cuzovic

Analysis of the Fatigue Behavior of 3D-Printed Maraging 300 Steel

Master's thesis in Produktutvikling og produksjon
Supervisor: Filippo Berto
June 2020

Norwegian University of Science and Technology
Faculty of Engineering
Department of Mechanical and Industrial Engineering



Kunnskap for en bedre verden

Preface

There has been a lot of insecurities regarding the purpose of this master thesis. Originally, the intention was to study additively manufactured test pieces made from 17-4 PH stainless steel made in the USA. However, as time went the test pieces were delayed and in the end it was not certain when they would arrive from the states. Instead, the material "Maraging 300 steel" additively manufactured in Norway was utilized.

From there on the purpose of the master thesis was to study the 3D printed Maraging 300 steel. The plan was to perform fatigue tests and porosity measurements, as well as the creation of graphs showing the material's fatigue behavior. Nanomechanical-, metallurgy- and fatigue test- laboratories needed to be used in order to make this possible. A lot of time went into getting access to these laboratories due to the need for courses, and laboratory training. Only the metallurgy laboratory training was complete and gained access to before the COVID-19 pandemic took root in Norway.

Due to the COVID-19 pandemic, NTNU had to close its campuses, and as a consequence it was not possible to use the laboratories, ultimately making it impossible to obtain experimental data on our own. The work had to be done from home. However, fatigue data, porosity images, and surface roughness images were obtained by PhD. candidate Klas Solberg before the closure of the campuses. The new plan was to plot and analyse the fatigue data that was retrieved before closure, measure the porosity, and compare these findings with articles that have done similar tests. The total amount of available material was the fatigue test data of two test specimens, 8 scanning electron microscope images of the fracture surface and surface roughness, and 1 optical microscope image of the porosity of one test specimen.

Abstract

Additive manufacturing (AM) is a manufacturing technology that can build structural parts made of metal through layer-by-layer build-up. The aim of this study is to investigate data from fatigue tests with two Maraging 300 steel specimens manufactured by selective laser melting (SLM), and to compare the data with existing studies that investigated the same material. One specimen is built horizontally, denoted as 0° build oriented, and the other specimen is built vertically, denoted as 90° build oriented. The surfaces on both test specimens underwent machining except for one surface on both specimens that remains as-built in order to observe the effect of surface roughness. Porosity image of the 90° (vertical) build oriented specimen is obtained, percent porosity is measured using python coding, and the percent porosity is compared with the porosity of the same material from existing studies. Finally, scanning electron microscope (SEM) images are obtained of both specimens in order to investigate the fracture surface and surface roughness.

List of Abbreviations

AM Additive manufacturing

CAD Computer aided design

CSV Comma-separated values

HIP Hot isostatic pressing

LOF Lack of fusion

LEFM Linear Elastic Fracture Mechanics

PH Precipitation hardenable

PNG Portable network graphics

SEM Scanning electron microscope

SLM Selective laser melting

SWT Smith Watson Topper

STEM Scanning transmission electron microscopy

TEM Transmission electron microscopy

W Watt

Contents

1	Introduction	1
1.1	Maraging 300 Steel	2
1.1.1	Heat Treatment	2
1.2	Systems of Additive Manufacturing	2
1.2.1	Powder Bed Systems	3
1.2.2	Powder Feed Systems	3
1.2.3	Wire Feed System	4
1.3	Selective Laser Melting	5
1.4	Factors that Influence Fatigue Behavior in AM Parts	5
1.4.1	Microstructure	6
1.4.2	Residual Stresses	6
1.4.3	Build Orientation	7
1.4.4	Rough Surface	8
2	Theory	9
2.1	Stress	9
2.2	Strain	9
2.3	Stiffness	9
2.4	Stress Amplitude	10
2.5	Fatigue	10
2.6	Fracture	10
2.7	SWT Parameter	11
3	Method	12
3.1	Plotting Graphs	13
3.2	Measuring Porosity	20
4	Results	21
4.1	Graphs for the Test Specimens	22

4.2	S-N Diagrams (Stress-Life Diagrams)	37
4.3	Porosity Results	41
4.4	Surface Roughness Results	41
5	Discussion	46
5.1	Analysis of the Graphs	46
5.2	S-N Diagrams	47
5.3	Analysis of the Porosity	48
5.4	Analysis of the Surface Roughness	49
6	Conclusion	50
	Bibliography	54
A	Coding	55

List of Tables

4.1	Number of black and white pixels, and the total number of pixels.	41
-----	---	----

List of Figures

1.1	Illustration of an AM powder bed system ⁸	3
1.2	Illustration of an AM powder feed system ⁸	4
1.3	Illustration of an AM wire feed system ⁸	4
1.4	To the left, an illustration of manufacturing an AM component and how the stair step effect is made. To the right, the as-built AM component with poor surface quality due to stair step effect that is caused by regions built with downward facing surfaces. ²⁶	8
3.1	(a) Specimen's dog bone shape with dimensions, and (b) thickness of the specimen.	12
3.2	(a) Horizontal specimen with a display of machined and as-built sides, and (b) vertical specimen.	13
4.1	Cycles vs. displacement graph of the 0° and 90° build oriented test specimens. Where (a) and (b) display the 0° build oriented specimen graph, while (c) and (d) display the 90° build oriented specimen graph.	22
4.2	Cycles vs. stiffness graph of the 0° build oriented test specimen.	23
4.3	Cycles vs. stiffness graphs of the 90° build oriented test specimen.	24
4.4	Cycles vs. stiffness graphs displayed with the upper part of the graph for both 0° and 90° build oriented specimens. Where (a) and (b) display the 0° build oriented specimen graph, while (c) and (d) display the 90° build oriented specimen graph.	25
4.5	Displacement vs. stress graph of the 0° build oriented test specimen.	26
4.6	Cycles vs. stress graph of the 90° build oriented test specimen.	27
4.7	Displacement vs. load graph of the 0° build oriented test specimen from start to fracture.	28
4.8	Graph displaying point intervals from the displacement vs. load graph for the 0° build oriented specimen.	29
4.9	Graph displaying point intervals from the displacement vs. load graph for the 0° build oriented specimen.	30

4.10	Displacement vs. load graph of the 90° build oriented test specimen from start to fracture of the specimen.	31
4.11	Graph displaying point intervals from the displacement vs. load graph for the 90° build oriented test specimen.	32
4.12	Graph displaying point intervals from the displacement vs. load graph for the 90° build oriented test specimen.	33
4.13	Strain vs. stress graph of the 0° build oriented test specimen.	34
4.14	Strain vs. stress graph of the 90° build oriented test specimen.	35
4.15	Time vs. displacement graphs of the (a) 0° and (b) 90° build oriented specimens.	36
4.16	Stress amplitude vs. number of cycles to failure.	37
4.17	Comparison between the stress amplitude vs. number of cycles to failure graph from this study with the study made by Meneghetti et al.. ¹⁴	38
4.18	SWT parameter vs. number of cycles to failure.	39
4.19	Comparison between the SWT parameter vs. number of cycles to failure graph from this study with the study made by Meneghetti et al.. ¹⁴	40
4.20	Original image compared to the binary image.	41
4.21	SEM images of (a) horizontally build oriented specimen section, and (b) vertically build oriented specimen section.	42
4.22	SEM images of the fracture surface of the 0° build oriented specimen at (a) 3 mm, (b) 1 mm, and (c) 500 μm	42
4.23	The marked surface roughness defect of the 0° build oriented specimen.	43
4.24	A view of defect size measurement of the 0° build oriented specimen.	43
4.25	SEM images of the fracture surface of the 90° build oriented specimen at (a) 3 mm, (b) 1 mm, and (c) 300 μm	44
4.26	(a) A view of defect size measurement of the 90° build oriented specimen, and (b) magnified view of the defect measurement.	45
5.1	Porosity measurements from the article by Adriano Fagali de Souza et al.. ⁷	48

Listings

3.1	Code for the cycles vs. displacement graph.	14
3.2	Code for the cycles vs. stiffness graph.	15
3.3	Code for obtaining the upper part of the cycles vs. stiffness graph.	16
3.4	Code for displaying the upper part and the normal cycles vs. stiffness graph together.	16
3.5	Code for the displacement vs. stress graph.	17
3.6	Code for the strain vs. stress graph.	17
3.7	Code for the time vs. displacement graph.	17
3.8	Code for the S-N diagram with stress amplitude and cycles to failure as parameters.	18
3.9	Code for the S-N diagram with SWT and cycles to failure as parameters.	19
3.10	Code for plotting the S-N diagrams from this study with S-N diagrams from existing studies.	19
3.11	Code for measuring the porosity.	20
A.1	Complete code for the cycles vs. displacement graph.	55
A.2	Complete code for the cycles vs. stiffness graph.	55
A.3	Complete code for obtaining the upper part of the cycles vs. stiffness graph.	56
A.4	Complete code for displaying the upper part and the normal cycles vs. stiffness graph together.	57
A.5	Complete code for the displacement vs. stress graph.	57
A.6	Complete code for the displacement vs. load graph.	58
A.7	Complete code for the stress vs. strain graph.	58
A.8	Complete code for the time vs. displacement graph.	59
A.9	Complete code for S-N diagram with stress amplitude vs. number of cycles to failure as parameters.	60
A.10	Complete code for comparing stress amplitude vs. number of cycles to failure graph between this study and existing studies.	61
A.11	Complete code for S-N diagram with SWT vs. number of cycles to failure as parameters.	62
A.12	Complete code for comparing SWT vs. number of cycles to failure graph between this study and existing studies.	63
A.13	Complete code for measuring porosity.	64

A.14 Complete code for displaying the original porosity image vs. the binary image. 64

1 Introduction

Additive manufacturing (AM) is a manufacturing method where material is added layer-by-layer creating the desired component with the assist of computer aided software such as CAD. This allows for topology optimized geometries and internal structures that would otherwise not be possible through conventional methods (e.g. machining).^{25 26 28} AM is used for many purposes, such as prototype making, tools, patterns, and concept parts among other uses. Parts made through AM can also be used directly as a functional part, however, the part needs to fulfil the required properties.⁹ According to Klas Solberg et al.,²⁸ examples where AM is being employed is for industries such as aerospace, medical, energy, and automotive.

However, the challenge regarding AM components is that they exhibit unfavorable properties in their as-built state, while conventionally built components do not exhibit these properties. In the article “What is going on with fatigue of additively manufactured metals?” by Klas Solberg and Filippo Berto²⁷ it is mentioned that the unfavorable properties normal for as-built components are reduction in fatigue life, reduced strength, reduced elongation at failure, high surface roughness, defects, anisotropic microstructure, and residual stresses. It is possible to increase the fatigue strength of AM components to the level of wrought components by utilizing post-processing treatments that alleviate the defects that causes reduced fatigue strength in AM components.²⁷

The post-processing methods that improve the fatigue performance of AM components are machining and heat treatments. Machining removes the defects that exist on the surface of the component, such as rough surfaces and other defects in the surface region. This leads to fewer points where the stress can concentrate, which makes it harder for crack initiation to occur. Heat treatments are effective for removing interior stresses, such as residual stresses, and alter the microstructure of the material. Also, internal pores can be closed by using hot isostatic pressing (HIP), which utilizes a combination of pressure and heat.²⁷

In this study, Maraging 300 steel is the investigated material. Two test specimen made from this material are 3D printed, one is built horizontally which will be denoted as 0° build oriented, and the other is built vertically and denoted as 90° build oriented. These test specimens underwent uniaxial ($R = 0$) load controlled fatigue testing, and the data from this test is then used to find displacement, stiffness, and stress of the test specimen.

The data is also used for comparison of values between this study and another article by Meneghetti et al.¹⁴ that has done similar studies with the same material. Image of porosity is taken in order to measure the percent porosity, and scanning electron microscope (SEM) images of the two test specimen are taken in order to investigate the surface roughness and fracture surfaces. The porosity in this study is compared with the porosity measurements from the article written by Adriano Fagali de Souza et al.⁷ where the effect of laser speed and layer thickness on the porosity is studied.

1.1 Maraging 300 Steel

Maraging steel is the investigated material in this study. It is an ultra-high-strength material which is made of carbon free iron-nickel alloys with addition of cobalt, molybdenum, titanium and aluminium. Depending on the type, the Maraging steels have a yield strength between 1400 and 2400 MPa. This steel is widely used in aerospace, e.g. undercarriage parts and wing fittings, tooling and machinery, and in ordnance components and fasteners due to its high strength combined with exceptional toughness properties and weldability.¹⁰

1.1.1 Heat Treatment

Aging heat treatment is standard for Maraging steels as it leads to the precipitation of intermetallic particles, and gives the material the desired properties such as good strength and toughness.^{11,29} The parameters that have a significant influence on the mechanical properties of the material are the aging temperature and time.²⁹ In this study the test specimen underwent heat treatment where they were exposed to direct aging at 500 °C for 5 hours. There is a risk with heat treating the material for a prolonged time at elevated temperatures as this leads to overaging. Overaging means that reversion of metastable martensite and coarsening of the intermetallic precipitates occur, which result in the decrease of hardness of the material.¹¹

1.2 Systems of Additive Manufacturing

There are many systems of additive manufacturing, in order to keep it simpler the manufacturing systems are divided into three broad categories: powder bed systems, powder feed systems, and wire feed systems.⁸

1.2.1 Powder Bed Systems

In the review of metal additive manufacturing by William E. Frazier,⁸ it is explained that in powder bed systems the powder is raked across the work area creating a powder bed. Then an energy source (electron beam or laser beam) delivers energy to the surface of the newly raked bed melting or sintering the powder into the desired shape. Then new powder is raked across the work area and the energy source melts or sinters the new powder. This process is repeated until the solid component is made. This manufacturing system enables the production of high resolution features, internal passages, and maintaining dimensional control.⁸

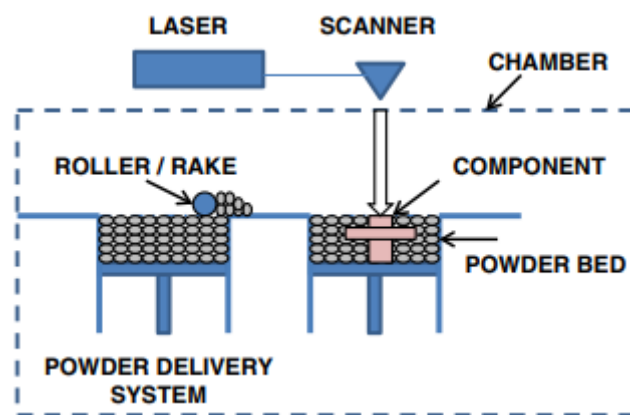


Figure 1.1: Illustration of an AM powder bed system⁸

1.2.2 Powder Feed Systems

Powder feed systems are different from powder bed systems in that they convey powders through a nozzle onto a build surface, and then an energy source such as a laser melts a mono-layer or more of the powder into the desired shape, and by repeating this process a solid component is made. There are two distinct advantages of the powder feed system, one is the systems ability to build larger volume scale more easily, and the other advantage is its useful ability to restore worn or damaged components.⁸

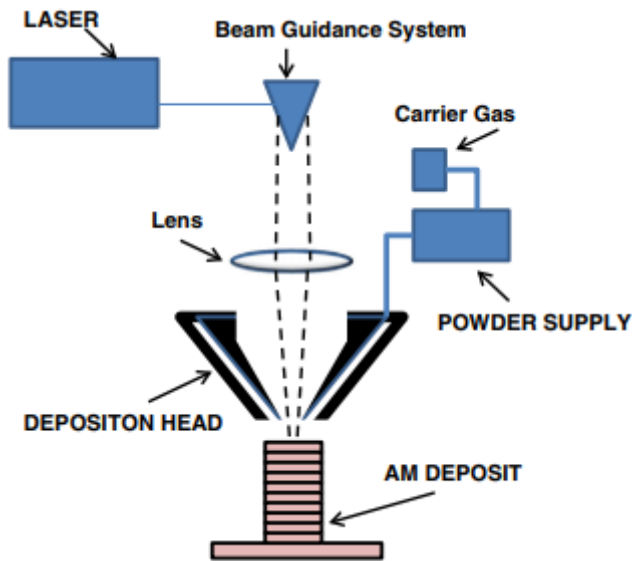


Figure 1.2: Illustration of an AM powder feed system⁸

1.2.3 Wire Feed System

In wire feed systems a wire is used as the feed stock and it is melted by an energy source that can be either electron beam, laser beam, or plasma arc. A solid component is built by firstly depositing a single bead of material and after several passes of such beads, it is built upon and in the end, the component is made. The advantages of the wire feed system is that it is well suited for high deposition rate processing and can create large build volumes; however, the disadvantage is that the fabricated component needs more after treatment such as machining compared to components made from powder bed or powder feed systems.⁸

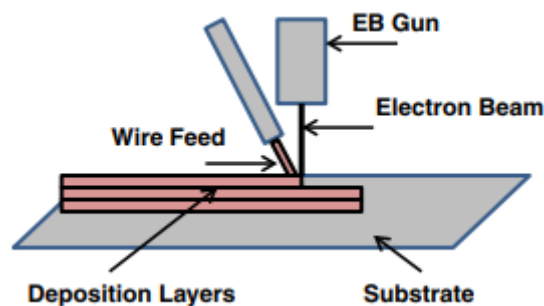


Figure 1.3: Illustration of an AM wire feed system⁸

1.3 Selective Laser Melting

The specimens in this study are made through selective laser melting (SLM). SLM falls into the powder bed systems category, where the part is built by spreading metal powder across a build platform and a laser beam selectively melts that powder layer-by-layer until a complete part is made. Process parameters such as laser power, scan speed, layer thickness, scanning space, laser diameter, focal distance, powder size, and powder temperature can influence the material properties in SLM processed parts. Adjusting these parameter alters the microstructure in the part, other factors that are important for the process parameters are the used materials, machine types and build volumes. An important element for the AM parts is the surface roughness, which is strongly affected by the variation of process parameters, more specifically the scanning speed, scan spacing and laser power. The advantages SLM processes have over other AM technologies is that SLM utilizes the metal powder as support for the build while other AM processes utilize some form of support material that is built separately. Additionally the powder is recyclable. The disadvantage of SLM processes is the need for stiff attachments from the parts onto the base plate in the build platform in order to minimize distortion in the part made by residual thermal stresses. After treatment such as machining or cutting are needed to remove the stiff attachments from the AM part.²⁰

1.4 Factors that Influence Fatigue Behavior in AM Parts

AM technologies show a lot of potential and uses in various industries, however, there are factors that create uncertainty about utilizing AM processed parts. According to Nima Shamsaei et al.²³ the factors that significantly influence the mechanical behavior of AM parts are material anomalies such as lack of fusion (LOF) voids, entrapped gas pores, microstructural properties, and heterogeneity that occur during the AM process due to directional heat transfer. In this study the specimens are made through SLM, a powder bed type system, and it is important to note that in powder bed systems there are two common manufacturing induced defects. One defect is the lack of fusion (LOF) voids which stem from partially- or un-melted powder particles, the other defect are pores that stem from entrapped gas. These defects are undesired as they are considered to be the key reason for the lower fatigue resistance of AM parts compared to the parts that are built conventionally. Fatigue crack initiation can occur due to the defects acting as micro-notches that cause stress concentrations and local plastic deformation on the interior of the material. In order to increase the fatigue resistance of the AM parts, hot isostatic

pressing (HIP) is utilized which reduces the internal defects by applying the combination of high pressure and high temperature. However, factors such as the material used and HIP parameters have significant influence on the process efficiency to eliminate defects, and some defects such as voids that are located close to the surface might not be removed as the HIP process cannot completely remove these defects.²³

There are also other obstacles that influence the fatigue performance of AM parts besides the aforementioned internal process induced defects, such as surface finish conditions, design parameters which include e.g. build orientation, process time interval, size, geometry and more, as well as residual stresses and high cycle fatigue behavior.²³

1.4.1 Microstructure

The microstructure of the AM part is a significant element that affects the fatigue behavior of the parts. Differences in the microstructure as well as the defects caused by different fabrication process parameters are crucial factors. It is the thermal history during the fabrication of the part, which are the heating and cooling rates, temperature gradient, and cyclic reheating, that affects how the microstructure is shaped. By adjusting these thermal parameters the amount, type, and distribution of internal defects can be influenced. However, it is the cooling rate that controls the microstructure, and the creation of defects does not influence the shape of the microstructure.¹⁵

The study by Reza Molaei et al.¹⁵ states that the most ordinary defects that causes fatigue crack initiations in AM parts are pores that are a result of entrapped gas, and lack of fusion (LOF) voids. The porosity in AM parts are highly affected by the processing parameters, which include scanning speed, hatch spacing, laser power, and focus distance with scan velocity and laser power being the parameters that have the most significant influence on the making of pores.¹⁵

1.4.2 Residual Stresses

According to N.S. Rossini et al.,²² residual stresses are the stresses that remain inside a material or body after manufacturing when no external forces or thermal gradients act on it.²² There are commonly three types of classifications of residual stresses denoted as types I, II, and III, which depend on the scale the stresses operate on. Type I residual stresses are the stresses that operate in the macro-scale, these stresses extend over a large range and are an important part of the distortion of material.²³ Type II and type III residual stresses are much smaller stresses. The difference between type II and III is that type II

stresses occur between grains at micro-scale, while type III stresses occur within grains at atomic-scale due to the presence of dislocations and other crystalline defects.^{22,23}

Development of residual stresses in AM parts generally occur during the fabrication process because of the rapid heating/cooling rates, significant spatially varied thermal distribution, and repeated tempering during succeeding laser-deposition process. Localized deformation is a common result of residual stresses, which can affect the strength and fatigue resistance of parts. It can deform the part's geometries, or possibly lead to failure of the part during fabrication.²³

Various methods are utilized in order to relieve residual stresses in AM parts, examples such as lowering the local thermal gradient during fabrication of the part by calibrating process parameters, maintaining optimal melt pool size, or pre-heat the build plate are regular methods. Post-processing methods are also applied in order to reduce residual stresses, they include post-process heat treatment, shot-peening, and surface rolling.²³

1.4.3 Build Orientation

Build orientation is an important element for AM parts as it affects the mechanical behavior. The thermal history of the manufacturing process is an important factor that affects the anisotropic behavior of AM parts as it can influence the direction and shape of defects in the material.¹⁵

The study made by Meneghetti et al.,¹⁴ shows that there is no difference in terms of mechanical properties between specimens that are built in vertical build orientation, and horizontal build orientation, for both as-built and heat treated specimens. However, regarding elongation after fracture, it is shown through axial fatigue tests that the lowest fatigue strength occurs for vertically built specimens. Fatigue strength of not heat treated vertically build oriented specimens was moderately lower than the heat treated specimens with the same build orientation, while for the horizontally build oriented specimens there was no indication in the results that show any major difference between the heat treated and not heat treated specimens. The same study performed a comparison between the test results, and data obtained from the literature and the fatigue testing of vacuum melted Maraging 300 steel that underwent annealing and annealing with age hardening. The comparison shows that both vertically and horizontally build oriented specimens that are not heat treated have 72% and 33% lower fatigue strength compared to vacuum melted Maraging in annealed condition, respectively. While the vertically and horizontally build oriented specimens that are heat treated have 68% and 61% lower fatigue strengths com-

pared to vacuum melted Maraging in annealed followed by age hardening condition, respectively.¹⁴

1.4.4 Rough Surface

Surface roughness is a vital factor that affects the fatigue behavior of AM parts. The reason why rough surfaces are important is because rough surface, as well as micro cracks, are potential areas for crack initiation, which lead to early fracture under cyclic loading. These rough surfaces on AM parts stem from the stair stepping effect that is caused by the curvature of the surface and the deposited layer thickness, partially melted particles, and the presence of material defects.¹⁵

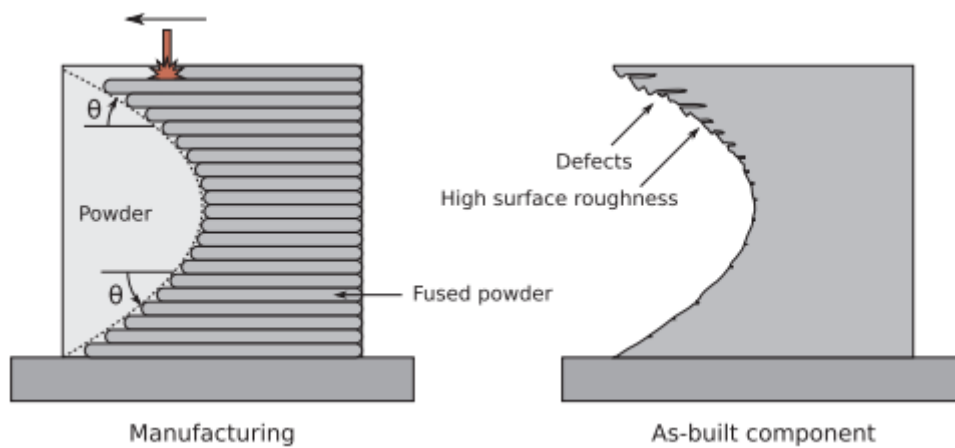


Figure 1.4: To the left, an illustration of manufacturing an AM component and how the stair step effect is made. To the right, the as-built AM component with poor surface quality due to stair step effect that is caused by regions built with downward facing surfaces.²⁶

2 Theory

The goal of this study is to investigate data from fatigue tests with two test specimens made from Maraging 300 steel manufactured through SLM, and to compare the data with existing studies that investigated the same material. We will also measure percent porosity and compare the result with existing studies, and investigate the surface roughness and fracture surface. The theory is presented in order to understand the method of how the data was investigated and compared with existing literature, and to give a general understanding of what can cause AM specimens to fail. The study has defined the following: stress, strain and stiffness of materials, stress amplitude, fatigue, fracture, and Smith Watson Topper (SWT) parameter.

2.1 Stress

Stress is force divided by area.¹⁹

$$\sigma = \frac{Force}{Area} \quad (2.1)$$

An external force is acting on a body and the resistance of the body represents the stress. In this study the type of stress is the engineering stress, which means that the area is the original cross-section area (A_0).¹⁹

2.2 Strain

The strain is the change in displacement divided by the direction of the displacement. The $d\mu$ is denoted as the change in displacement, while dx is the direction of the displacement.¹⁹

$$\varepsilon = \frac{d\mu}{dx} \quad (2.2)$$

”Strain is also a measure of deformation of the material based on a reference length.” (Nestor Perez, Fracture Mechanics, 2).¹⁹

2.3 Stiffness

The basic definition of stiffness is load divided by deformation.⁶ Stiffness is the incline in the load and deformation relationship.¹⁶ This definition includes that the deformation

is caused by the load. It is important to have the precise load configurations and precise deformation.⁶

$$Stiffness = \frac{Load}{Deformation} \quad (2.3)$$

2.4 Stress Amplitude

In cyclic loads, constant and/or variable stress amplitudes are required to cause fracture. The stress amplitude is measured by taking the maximum stress subtracting it with the minimum stress and dividing by 2.¹⁷

$$\sigma_a = \frac{\Delta\sigma}{2} = \frac{\sigma_{max} - \sigma_{min}}{2} \quad (2.4)$$

In natural environments, the component is subjected to numerous different stresses, some of them are constant stress amplitudes and others are variable stress amplitudes.¹⁷ In this study the stress amplitude is constant as it is performed under a controlled environment.

2.5 Fatigue

Fatigue in a material is considered a form of failure which is caused by repeated cyclic loading for a period of time, meaning that the fatigue is dependent on the time. The failure is defined as progressive as it starts as crack initiation, denoted as stage I. These cracks can be microscopic, and this stage consumes many cycles before crack growth initiates. The crack growth stage denoted as stage II is where many grains are deformed and the crack grows in the direction of local principal stress. The crack continues to grow until it reaches a critical size. This is when the final stage, stage III called crack propagation or instability stage begins. This is the stage where the crack grows fast and ultimately the fracture occurs.¹⁷

2.6 Fracture

”Fracture mechanics is the study of mechanical behavior of cracked materials subjected to an applied load.” (Nestor Perez, Fracture Mechanics, 53).¹⁸ Formation of cracks, crack growth, and rupture process is what the fracture mechanics is about. Microstructure is an important factor for the formation of cracks and the fracture process, since the microstructural features are imperfections and can act as fracture initiation. These features are precipitates, inclusions, grain size, and the phases that make up the microstructure.¹⁸

2.7 SWT Parameter

The Smith Watson Topper (SWT) is a stress-strain function (for use in metal fatigue) that takes the effect of mean stress into account, and is also useful in high cycle fatigue and low cycle fatigue test.^{12 24}

In this study, an alternate form of the SWT parameter is used. This alternate form is used when stresses are approximately proportional to strains.²⁴

$$SWT = \sqrt{\sigma_{max}\sigma_a} \quad (2.5)$$

3 Method

The aim of this thesis is divided into three parts, one part is to analyse experimental data related to AM manufacturing and to compare the data with existing studies that investigate the same material. Another part is to measure the percent porosity of one test specimen and to compare the porosity with existing studies that measure the porosity of the same material. Lastly we will investigate the fracture surface and surface roughness of the specimens using SEM images. The experimental data from the fatigue test and the images of the surface roughness and the porosity used in the thesis was obtained by my co-supervisor Klas Solberg.

Two dog bone shaped test specimens made of maraging 300 steel have been additively manufactured through SLM by using a laser power of 180 W, hatch spacing of 0.105 mm, scan velocity of 650 mm/s, and layer thickness of 30 μm . The geometry of the test specimen is shown in figure 3.1. One test specimen is built horizontally, while the other is built vertically. In this thesis, the horizontal specimens are denoted as 0° build oriented specimen, and the vertical specimens are denoted as 90° build oriented specimen, see figure 3.2. This is in order to avoid confusion when comparing the specimens from this study with specimens from other studies. The test specimens also underwent heat treatment in the form of direct ageing of $500^\circ C/5h$. It is important to note that both test specimens have one part of the surface that is as-built while the rest of the surfaces are machined, as displayed in figure 3.2. This is in order to observe the effect of the surface roughness.

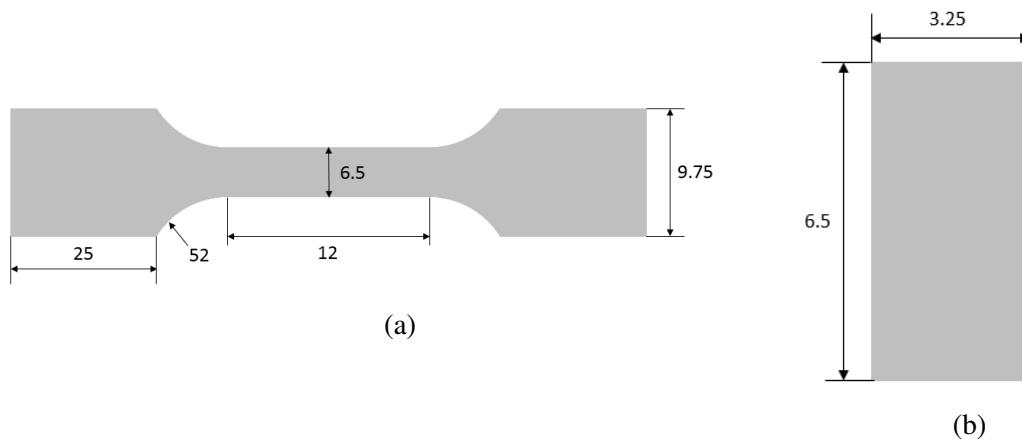


Figure 3.1: (a) Specimen's dog bone shape with dimensions, and (b) thickness of the specimen.

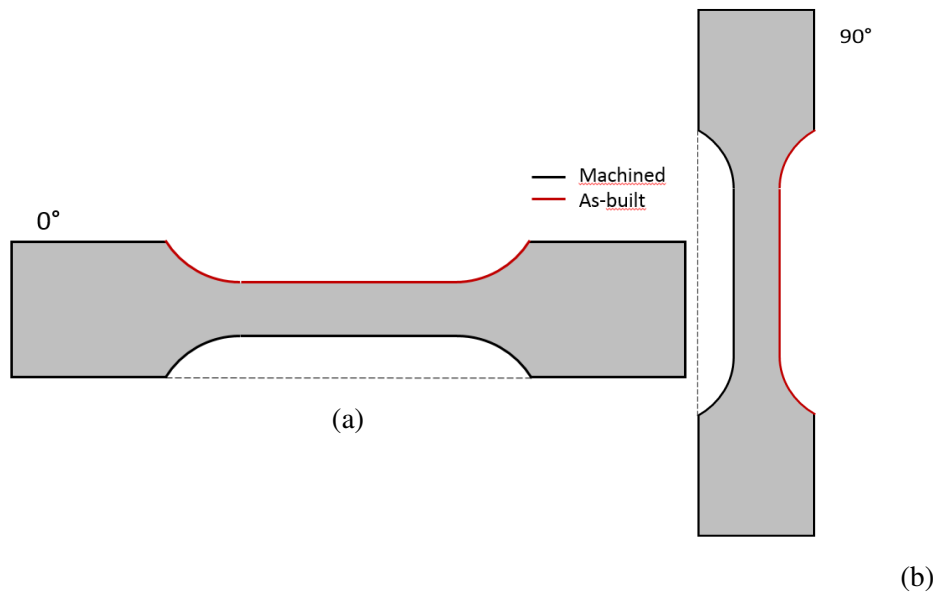


Figure 3.2: (a) Horizontal specimen with a display of machined and as-built sides, and (b) vertical specimen.

Uniaxial ($R = 0$) load controlled fatigue test with a frequency of 30 Hz on the Servo hydraulic MTS system with 50 kN load cell were carried out on the dog bone shaped specimens. Surface roughness images of both the test specimens were taken using the scanning electron microscope (SEM) machine, Quanta FEG 650. Porosity images of the 90° build oriented (vertical) specimen were obtained by first cutting a small piece of the specimen and then polishing it using coarse sandpaper to begin with then progressively using finer sandpaper. After polishing, the piece is put under a optical microscope where the images are taken in the XZ plane at 5 times zoom (unfortunately the scale bar is not visible in the image). Lastly, python programming was utilized to plot the data from the fatigue test onto graphs, plot the S-N diagrams, and to measure the percent porosity of the vertical specimen by using the porosity image. Additionally, a tool used for extracting data from plots and images called "Web plot digitizer"¹ is utilized to measure the size of the defects from the SEM images, and to merge S-N diagrams from this study with existing studies in order to compare data.

3.1 Plotting Graphs

The graphs were plotted using Jupyter Notebook,² an open-source web application that supports Python programming language, which is the programming language used for plotting the graphs. Data for both the 0° and 90° test specimens were obtained from

the fatigue tests. These data consist of running time, axial load, axial displacement, and number of cycles. Firstly, the data was converted into CSV files in order to be read in Python using "pandas",³ a powerful data analysis and manipulation tool, built on top of the Python programming language. After reading the data, it is then plotted using "Matplotlib",⁴ a visualization tool in Python.

The graphs consist of cycles vs. displacement, cycles vs. stiffness and the upper part of this graph, cycles vs. stress, displacement vs load, strain vs stress, time vs displacement, and S-N diagrams. Listing 3.1 shows the code for the cycles vs. displacement graph, which has many lines of codes that are necessary for the other codes as well. The lines are as follows:

- Lines 1-3 are importing the necessary tools, "matplotlib.pyplot", "pandas", and "numpy"⁵ a scientific computing tool for Python, and naming them "plt", "pd", and "np", respectfully.
- Line 5 is reading the CSV file "data-0.csv", which is the data for the test specimen built in 0° build orientation, with the "pandas" tool. This allows the code to utilize the data from the CSV file so that it can be plotted.
- Line 7 determines the figure size, while line 9 determines the figure title as well as the size and style of the title.
- Line 11 utilizes the data and plots the number of cycles in the x-axis and the displacement in the y-axis using the "matplotlib.pyplot" tool.
- Lines 13 and 14 displays the x- and y-labels.
- Line 16 displays the legend in the graph.
- Lines 19-21 limits the axis, showing only the desired values e.g. values from 0 to 100
- Line 23 saves the graph as a PNG file, while line 25 displays the figure.

```
1 import matplotlib.pyplot as plt
2 import numpy as np
3 import pandas as pd
4
5 data = pd.read_csv('data-0.csv', sep=";")
6
7 plt.figure(figsize=(5.9, 5))
```

```

8
9 plt.title('Cycles vs Displacement', fontdict={'fontweight': 'bold', '
    fontsize': 18})
10
11 plt.plot(data.cycles, data.mm, '-')
12
13 plt.xlabel('Cycles')
14 plt.ylabel('Displacement')
15
16 plt.legend()
17
18 #Limiting the axis, showig e.g. values from 0 to 100.
19 # ax = plt.gca()
20 # ax.set_xlim([0,20])
21 # ax.set_ylim([0,0.25])
22
23 plt.savefig('Cycles_vs_displacement_0.png', dpi=300)
24
25 plt.show()

```

Listing 3.1: Code for the cycles vs. displacement graph.

The other codes will have similar coding with some differences. Therefore, the following codes will contain only the most important differences as to not display the same codes repeatedly. The full codes will be displayed in the appendix. Also, the codes for displaying data for the test specimen with 90° build orientation are identical with the exception of the code line for reading the CSV file, which needs to read the "data-90.csv" file.

The code displayed in listing 3.2 starts with reading the data, as it's done in the previous code. Stiffness of the test specimen is calculated in line 7 by dividing the load (kN) with the displacement (mm): $\frac{Load}{Displacement}$.

```

1 data = pd.read_csv('data-0.csv', sep=";")
2
3 plt.figure(figsize=(5.9,5))
4
5 plt.title('Cycles vs Stiffness', fontdict={'fontweight': 'bold', '
    fontsize': 18})
6
7 stiffness = (data.kN/data.mm)
8
9 plt.plot(data.cycles, stiffness, 'b-', label='kN/mm')
10

```

```

11 plt.xlabel('Cycles')
12 plt.ylabel('Stiffness')

```

Listing 3.2: Code for the cycles vs. stiffness graph.

The code shown in listing 3.3 displays the upper part of the cycles vs. stiffness graph. It was made in order to give a clearer estimate of how high the stiffness value became during the testing.

- Line 3 decides a maximum value.
- Line 4 makes it so that every stiffness value that is below the maximum value turns into the maximum value, which is 51 kN/mm.

```

1 stiffness = (data.kN/data.mm)
2
3 maxVal = 51
4 stiffness[stiffness < maxVal] = maxVal
5
6 plt.plot(data.cycles, stiffness, '-', label='kN/mm')

```

Listing 3.3: Code for obtaining the upper part of the cycles vs. stiffness graph.

The code shown in listing 3.4 is very similar to the previous code, except for that in this code both the normal cycles vs. stiffness graph and the upper part of said graph is plotted together.

```

1 stiffness = (data.kN/data.mm)
2
3 maxVal = 51
4 stiffness[stiffness < maxVal] = maxVal
5
6 stiffness_norm = (data.kN/data.mm)
7 cycles = data.cycles
8
9 plt.plot(data.cycles, stiffness, 'y-', linewidth=3, label='kN/mm')
10 plt.plot(cycles, stiffness_norm, '-', label='kN/mm', alpha=0.5)

```

Listing 3.4: Code for displaying the upper part and the normal cycles vs. stiffness graph together.

In the code shown in listing 3.5, surface area of the test specimen is calculated $length \times width$ which becomes: 6.5×3.25 , see figure 3.1. The stress ($\frac{force}{area}$) is then calculated by taking the load (data.kN) from the data and dividing it with the surface area of the test

specimen and multiplying it with 1000: $\frac{data.kN}{area} \times 1000$. It is multiplied with 1000 in order to get MPa [$\frac{N}{mm^2}$].

```
1 area = 6.5*3.25
2 stress = (data.kN/area)*1000
3
4 plt.plot(data.mm[:-8], stress[:-8], '--', label="MPa")
```

Listing 3.5: Code for the displacement vs. stress graph.

In the code shown in listing 3.6 it is important to find the stress and strain. The stress was found to be $\frac{data.kN}{area} \times 1000$, while the strain ($\frac{L-L_0}{L_0}$) is found by taking the estimation of the length $L_0 = 12mm$, see figure 3.1, and adding it to the displacement of the test specimen (data.mm):

$$\frac{((12 + data.mm) - 12)}{12}$$

```
1 area = 6.5*3.25
2 stress = (data.kN/area)*1000
3 strain = ((12+data.mm)-12)/(12)
```

Listing 3.6: Code for the strain vs. stress graph.

The code for displaying time vs. displacement graph shown in listing 3.7 is also straight forward. The time is made from seconds to minutes by dividing the time values with 60: $minutes = \frac{data.sec}{60}$.

```
1 minutes = data.sec/60
2
3 plt.plot(minutes[:-8], data.mm[:-8], '-')
```

Listing 3.7: Code for the time vs. displacement graph.

In the code for obtaining the S-N diagram of the cycles to failure vs. stress amplitude, shown in listing 3.8, it is necessary to obtain the maximum and minimum stress values for both the 0° and 90° test specimen data. This is done in lines 5-6 where the maximum and minimum stress value for both specimen is measured. The maximum stress value is measured by taking the maximum load, which is 10 kN, and dividing it with the area: $maximum\ stress = \frac{10000}{(6.5 \cdot 3.25)}$, giving a result of approximately 473 MPa. The minimum stress value is measured in the same way by taking the minimum load, which is 0 kN, and dividing it with the area. This gives a result of 0 MPa. Lines 8-9 give the total number of cycles for both specimen, which is 60760 cycles for 0° test specimen and 148339 cycles for 90° test specimen.

The stress amplitude is defined as:

$$\sigma_a = \frac{\sigma_{max} - \sigma_{min}}{2} \quad (3.1)$$

As shown in the book Fracture Mechanics (chapter: Fatigue Crack Growth) by Nestor Perez.¹⁷

Lines 11 and 14 calculate the stress amplitude:

$$\sigma_{a0^\circ} = \text{Stress amplitude for } 0^\circ = \frac{473 - 0}{2} \quad (3.2)$$

$$\sigma_{a90^\circ} = \text{Stress amplitude for } 90^\circ = \frac{473 - 0}{2} \quad (3.3)$$

```
1 area = 6.5*3.25
2 stress_0 = (data_0.kN/area)*1000
3 stress_90 = (data_90.kN/area)*1000
4
5 ymax = 10000/(area)
6 ymin = 0/(area)
7
8 x_xmax = data_0.cycles[np.argmax(data_0.cycles)]
9 x_xmax_90 = data_90.cycles[np.argmax(data_90.cycles)]
10
11 S_0 = (ymax-ymin)/2
12 N_0 = 60760
13
14 S_90 = (ymax-ymin)/2
15 N_90 = 148339
16
17 plt.loglog(N_0, S_0, 'r*', label='data-0')
18 plt.loglog(N_90, S_90, 'bx', label='data-90')
```

Listing 3.8: Code for the S-N diagram with stress amplitude and cycles to failure as parameters.

The code that obtains the S-N diagram of the cycles to failure vs. SWT parameter, shown in listing 3.9, is very similar to the last code except for that the SWT parameter needs to be measured. SWT parameter can be measured as:

$$\sqrt{\sigma_{max} \cdot \sigma_a} \quad (3.4)$$

As described in the article "A stress-strain function for the fatigue of metals" by K.N. Smith et al.²⁴

Lines 3 and 7 measures the SWT parameter by taking the square root of the maximum stress value, which was 473 MPa, multiplied with the stress amplitude:

$$SWT \text{ for } 0^\circ = \sqrt{473 \cdot \sigma_{a0^\circ}} \quad (3.5)$$

$$SWT \text{ for } 90^\circ = \sqrt{473 \cdot \sigma_{a90^\circ}} \quad (3.6)$$

```

1 S_0 = (ymax-ymin)/2
2 N_0 = 60760
3 SWT_0 = math.sqrt(ymax*S_0)
4
5 S_90 = (ymax-ymin)/2
6 N_90 = 148339
7 SWT_90 = math.sqrt(ymax*S_90)

```

Listing 3.9: Code for the S-N diagram with SWT and cycles to failure as parameters.

The code for plotting the S-N diagrams from this study together with the S-N diagrams from the study made by Meneghetti et al.¹⁴ is displayed in listing 3.10. The code is similar to the other S-N diagram codes except for that it also plots data obtained from the other study.

```

1 data_0 = pd.read_csv('data-0.csv', sep=";")
2 data_90 = pd.read_csv('data-90.csv', sep=";")
3
4 AD0NT = pd.read_csv('AD0NT.csv', sep=";")
5 AD0T = pd.read_csv('AD0T.csv', sep=";")
6 AD90NT = pd.read_csv('AD90NT.csv', sep=";")
7 AD90T = pd.read_csv('AD90T.csv', sep=";")
8
9 plt.loglog(N_0, S_0, 'r*', label='data-0')
10 plt.loglog(N_90, S_90, 'bx', label='data-90')
11
12 plt.loglog(AD0NT.X, AD0NT.Y, 'g^', label='90_NT')
13 plt.loglog(AD0T.X, AD0T.Y, 'yo', label='90_T')
14 plt.loglog(AD90NT.X, AD90NT.Y, 'ms', label='0_NT')
15 plt.loglog(AD90T.X, AD90T.Y, 'kD', label='0_T')

```

Listing 3.10: Code for plotting the S-N diagrams from this study with S-N diagrams from existing studies.

3.2 Measuring Porosity

Porosity measurements were carried out on Jupyter Notebook, using the Python programming language. Firstly, a SEM image of the 90° build oriented (vertical) specimen surface is read before the image is converted into a binary image, meaning it only consists of black and white pixels. The idea is that the black pixels represent the pores in the material while the white pixels represent the normal surface. Then it finds the total number of black and white pixels, as well as the total number of pixels in the image. Lastly the number of black pixels is divided with the total number of pixels in the image and multiplied with 100 to find the percentage of porosity:

$$\text{Percent porosity} = \frac{\text{Black pixels}}{\text{Total number of pixels}} \times 100 \quad (3.7)$$

The code shown in listing 3.11 reads the SEM image and converts it to a binary image, then finds the number of black and white pixels, and the total number of pixels in the image:

```
1 img = cv2.imread('Image_5652.tif', cv2.IMREAD_GRAYSCALE)
2 ret,thresh1 = cv2.threshold(img, 127, 255, cv2.THRESH_BINARY)
3 n_white_pix = np.sum(thresh1 == 255)
4 n_black_pix = np.sum(thresh1 == 0)
5 size = img.size
```

Listing 3.11: Code for measuring the porosity.

4 Results

The data obtained from the uniaxial ($R = 0$) load controlled fatigue tests are plotted and presented in section 4.1 for both the 0° (horizontal) and 90° (vertical) build oriented specimen, section 4.2 presents the plotted S-N diagrams, the porosity measurement is presented in section 4.3, and section 4.4 presents the surface roughness images of the two test specimens. Graphs are created in order to observe trends and changes in values, as well as for comparison purposes. S-N diagrams, porosity measurements and surface roughness are also created for the purpose of comparison, which will be discussed.

4.1 Graphs for the Test Specimens

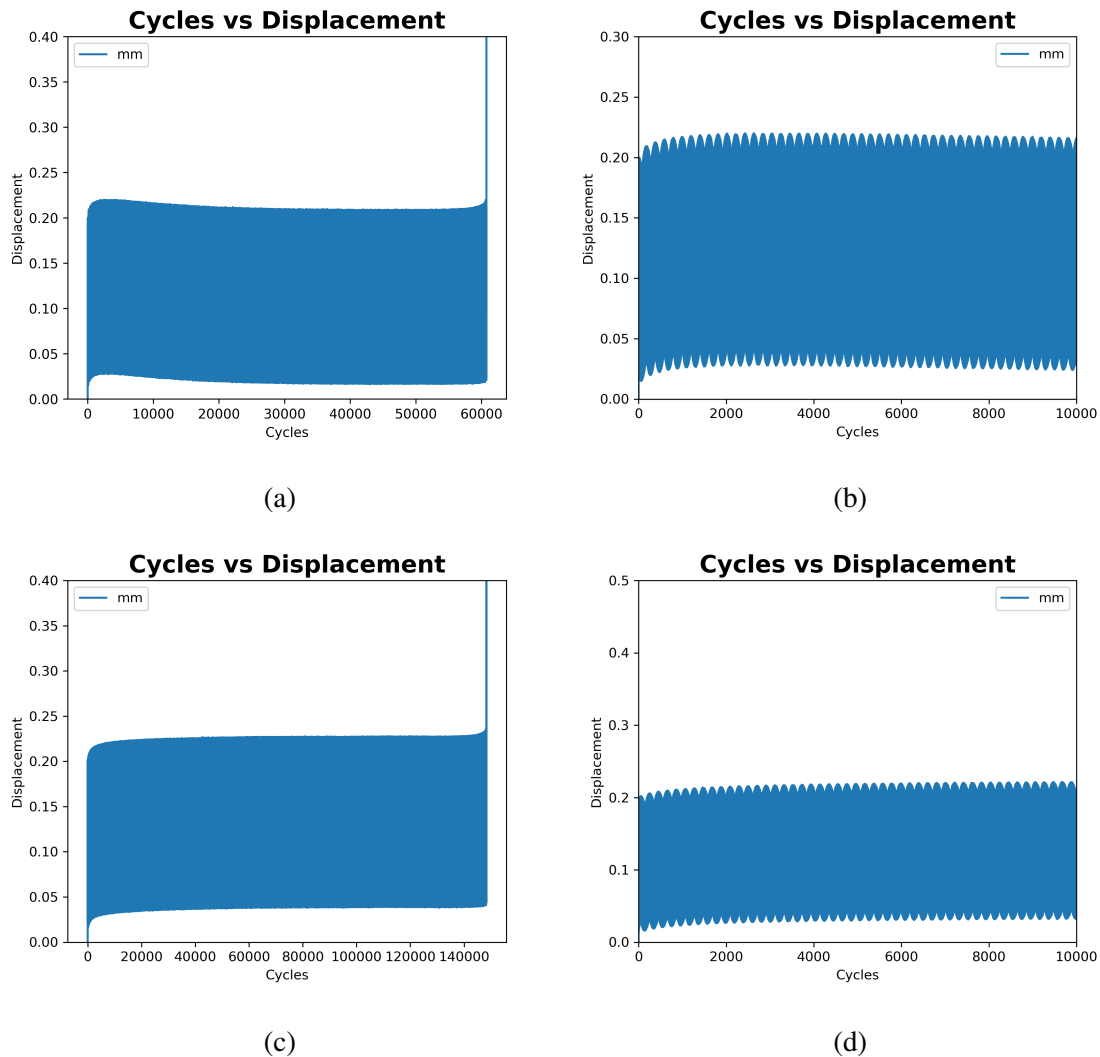


Figure 4.1: Cycles vs. displacement graph of the 0° and 90° build oriented test specimens. Where (a) and (b) display the 0° build oriented specimen graph, while (c) and (d) display the 90° build oriented specimen graph.

Figure 4.1 shows that the 0° build oriented test specimen lasts a little over 60,000 cycles before fracture occurs, and it has a relatively steady displacement over the course of the entire fatigue test. The displacement is a little over 0.2 mm and it gradually comes closer to the 0.2 mm length. The 90° build oriented test specimen lasts over 140,000 cycles before fracture occurs, and it also has a relatively steady displacement over the course of the entire fatigue test. The displacement is a little over 0.2 mm while gradually narrowing down to the 0.2 mm length.

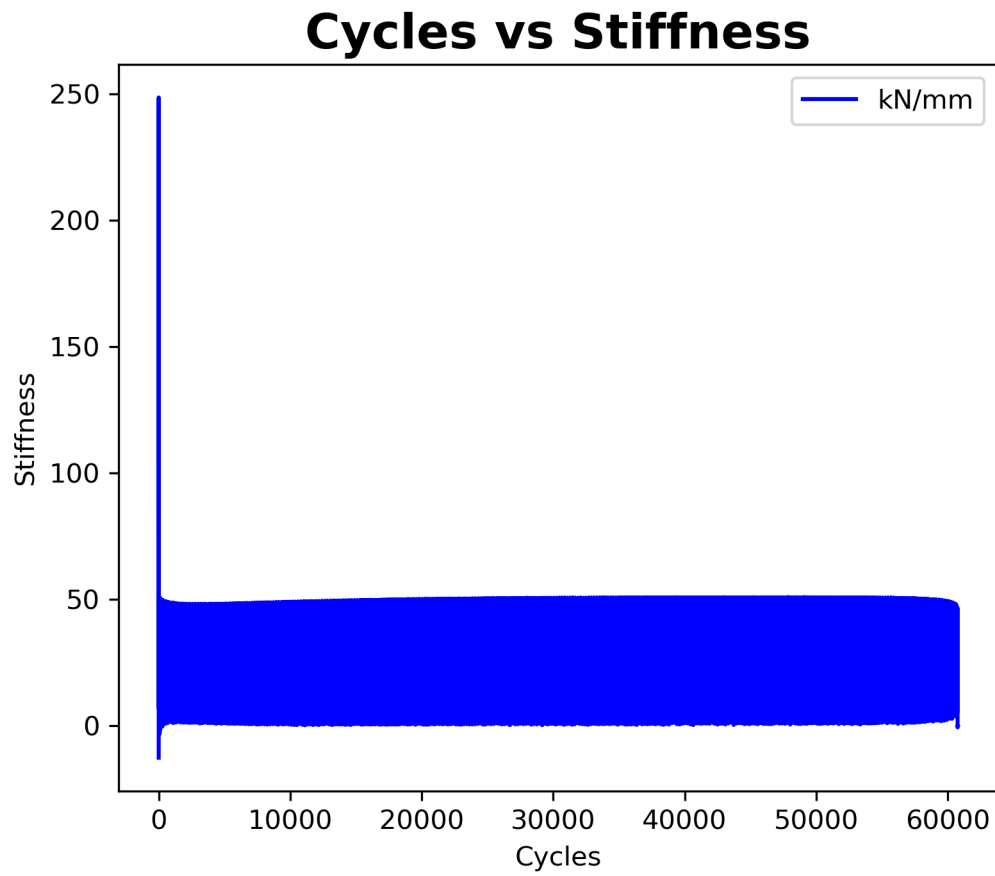


Figure 4.2: Cycles vs. stiffness graph of the 0° build oriented test specimen.

Figure 4.2 shows that the 0° build oriented test specimen has a relatively steady stiffness over the course of the test with the exception of at the start of the test. The stiffness measures a little over 50 $\frac{kN}{mm}$.

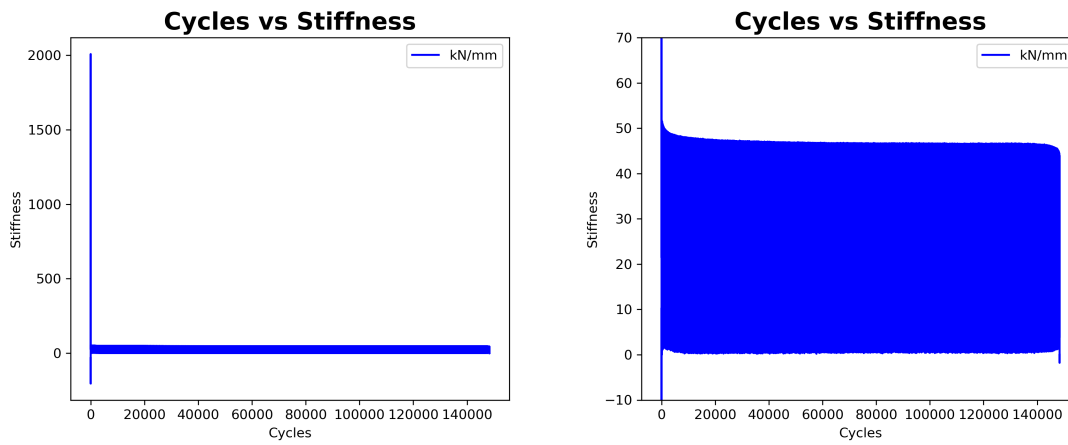
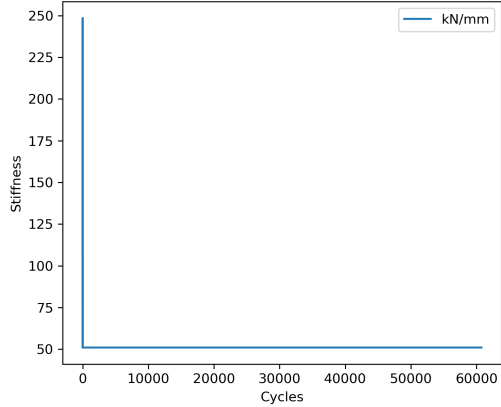


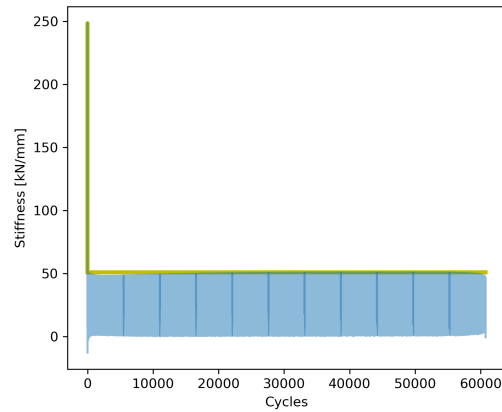
Figure 4.3: Cycles vs. stiffness graphs of the 90° build oriented test specimen.

Figure 4.3 shows that the 90° build oriented test specimen has a relatively steady stiffness over the course of the test with the start of the test as an exception. The stiffness measures approximately $50 \frac{kN}{mm}$.

The upper part of the cycles vs stiffness curve

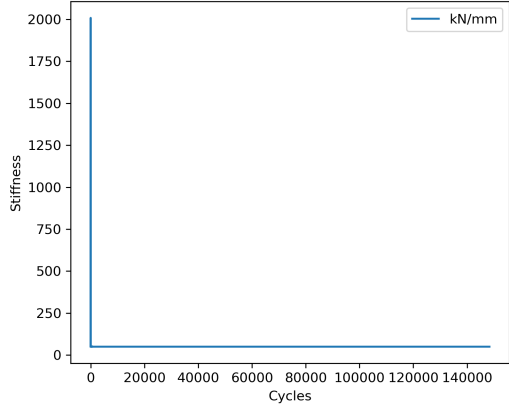


(a)

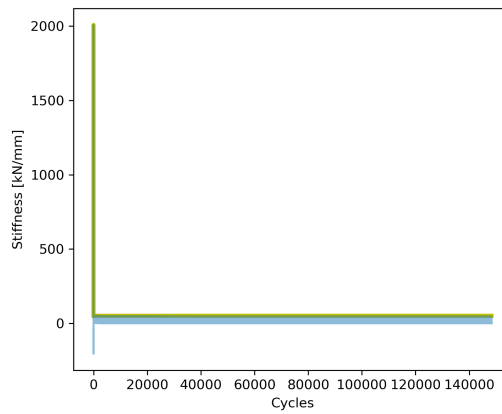


(b)

The upper part of the cycles vs stiffness curve



(c)



(d)

Figure 4.4: Cycles vs. stiffness graphs displayed with the upper part of the graph for both 0° and 90° build oriented specimens. Where (a) and (b) display the 0° build oriented specimen graph, while (c) and (d) display the 90° build oriented specimen graph.

Figure 4.4 displays the upper part of the curves for both 0° and 90° build oriented specimens in order to show the highest values of stiffness.

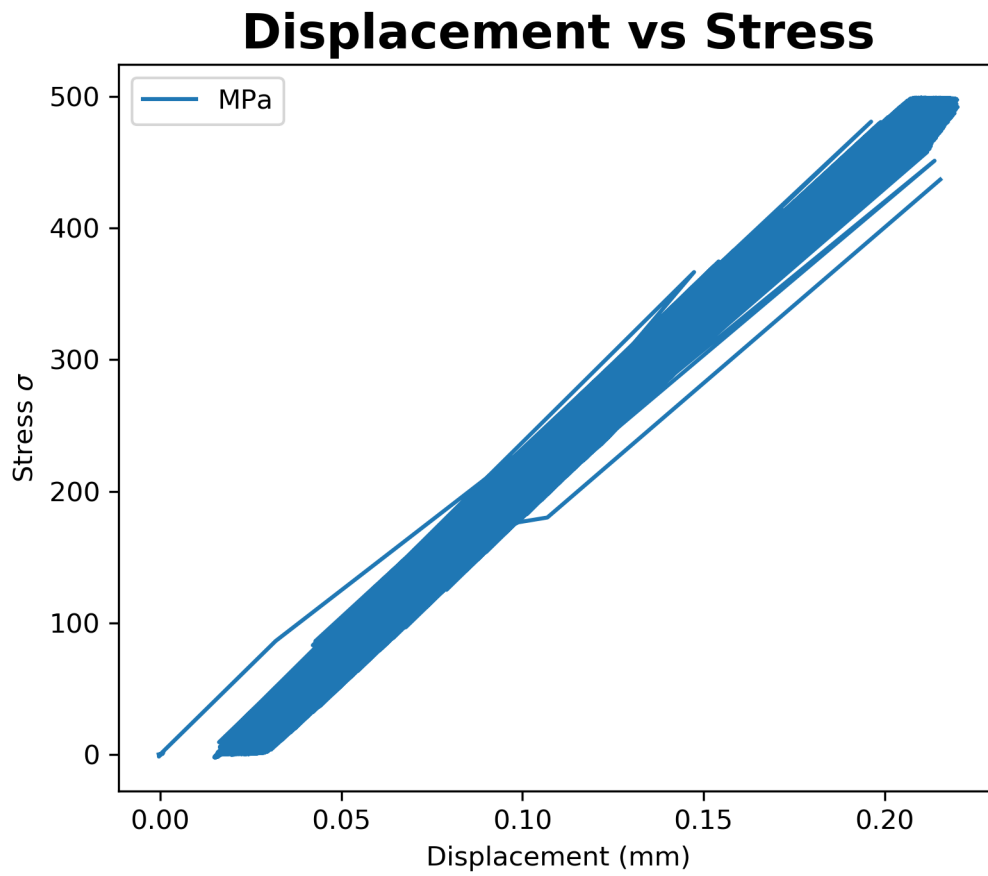


Figure 4.5: Displacement vs. stress graph of the 0° build oriented test specimen.

Figure 4.5 shows that for the 0° build oriented specimen the stress is roughly 500 MPa when the displacement is approximately 0.2 mm, and that the displacement becomes gradually larger.

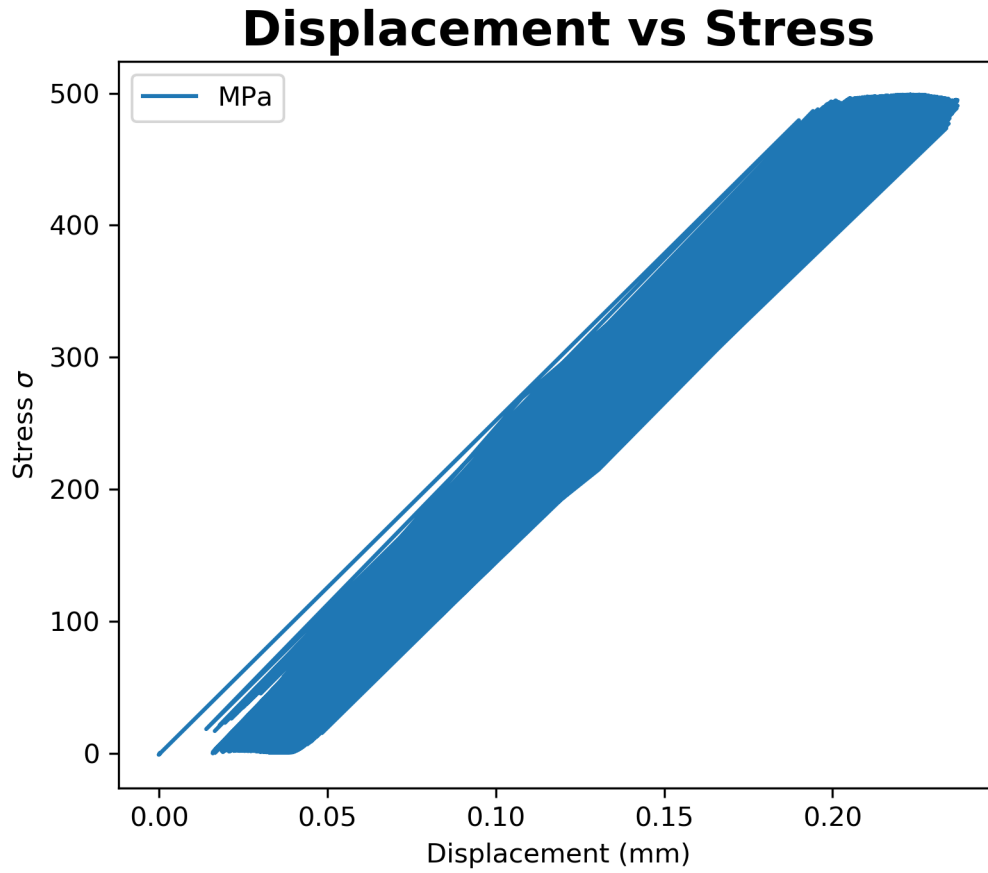


Figure 4.6: Cycles vs. stress graph of the 90° build oriented test specimen.

Figure 4.6 shows that for the 90° build oriented specimen the stress is roughly 500 MPa when the displacement is approximately 0.2 mm, and that the displacement becomes gradually larger.

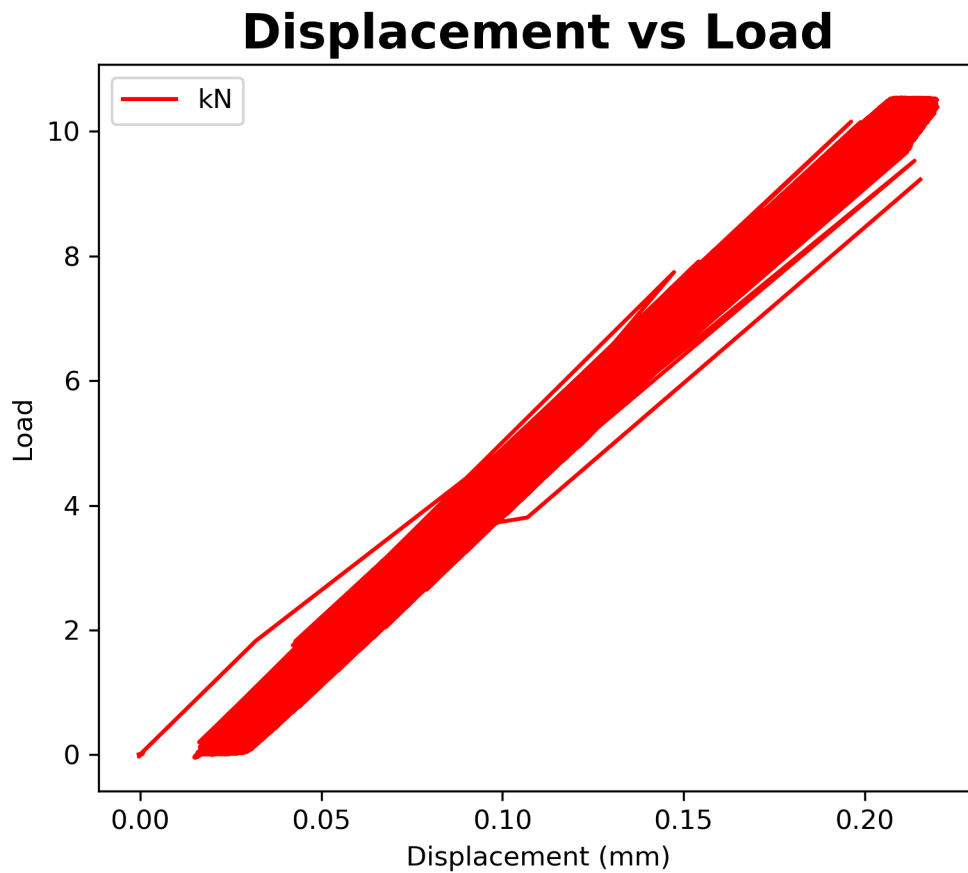


Figure 4.7: Displacement vs. load graph of the 0° build oriented test specimen from start to fracture.

Figure 4.7 shows the displacement vs. the load of the 0° build oriented test specimen. The maximum load is roughly 10 kN and the largest displacement is around 0.2 mm. This figure also shows a stiffness trend as the slope of the curve is the stiffness.

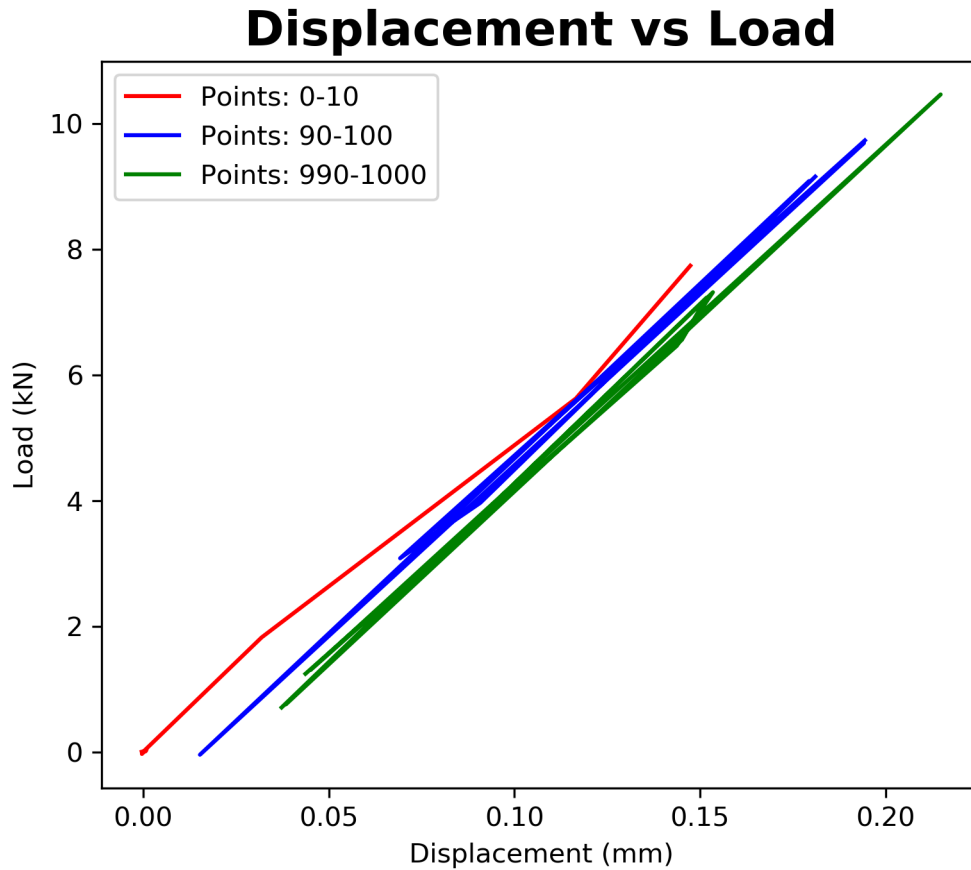


Figure 4.8: Graph displaying point intervals from the displacement vs. load graph for the 0° build oriented specimen.

The stiffness trend is displayed more clearly in figure 4.8 where the red line represents the interval for points 0 to 10 (the first 10 points in the graph). The blue line represents the interval for points 90 to 100, and lastly the green line represents the interval for points 990 to 1000.

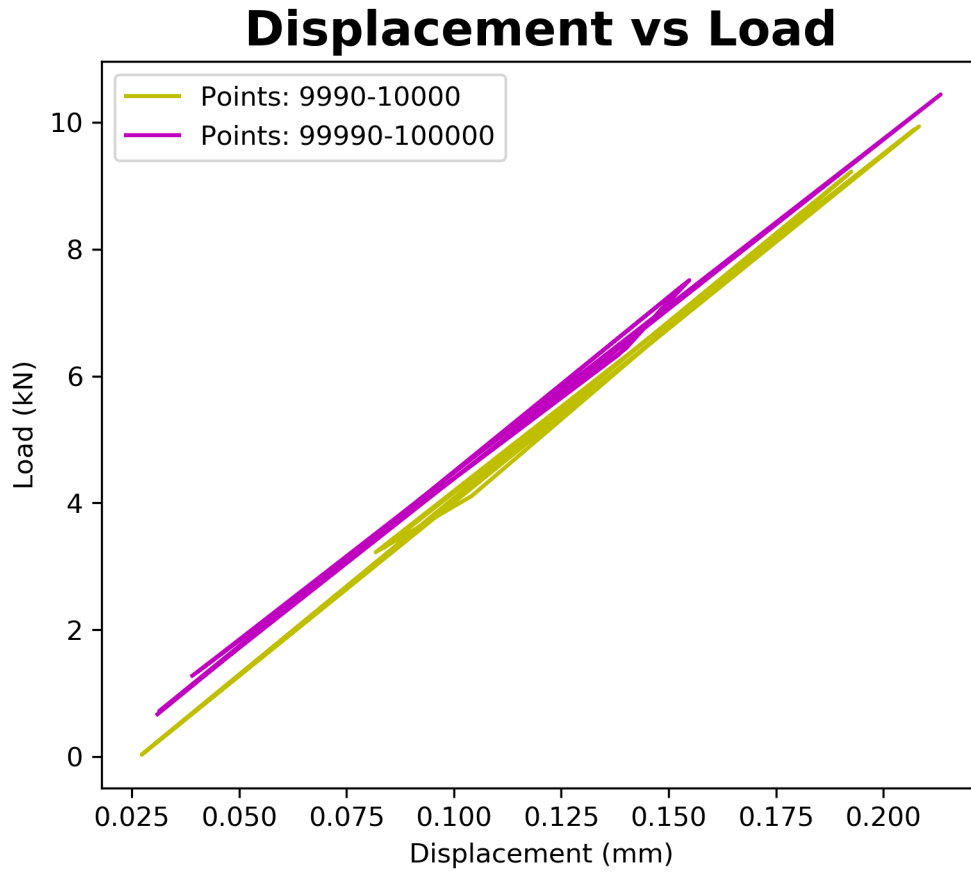


Figure 4.9: Graph displaying point intervals from the displacement vs. load graph for the 0° build oriented specimen.

When approaching the end of the fatigue test however, the interval for points 99,990 to 100,000 is behind the interval for points 9,990 to 10,000 as shown in figure 4.9.

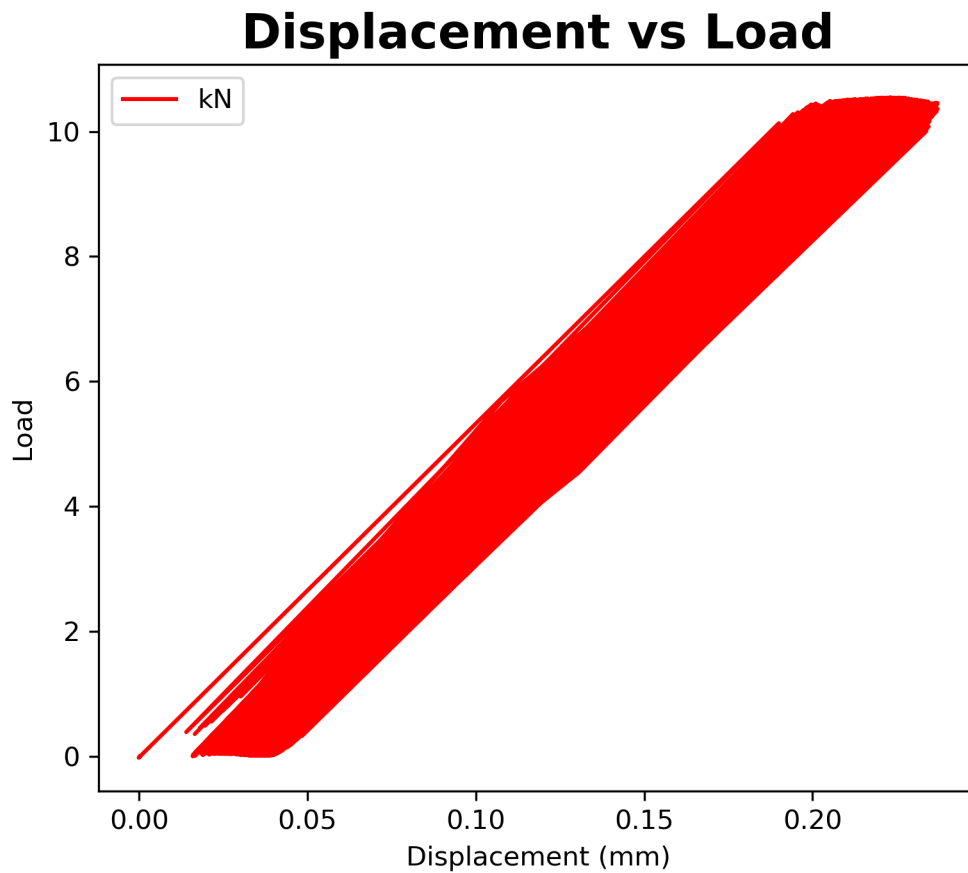


Figure 4.10: Displacement vs. load graph of the 90° build oriented test specimen from start to fracture of the specimen.

Figure 4.10 shows the displacement vs. the load of the 90° build oriented test specimen. The maximum load is roughly 10 kN and the largest displacement is around 0.2 mm. This figure also shows a stiffness trend.

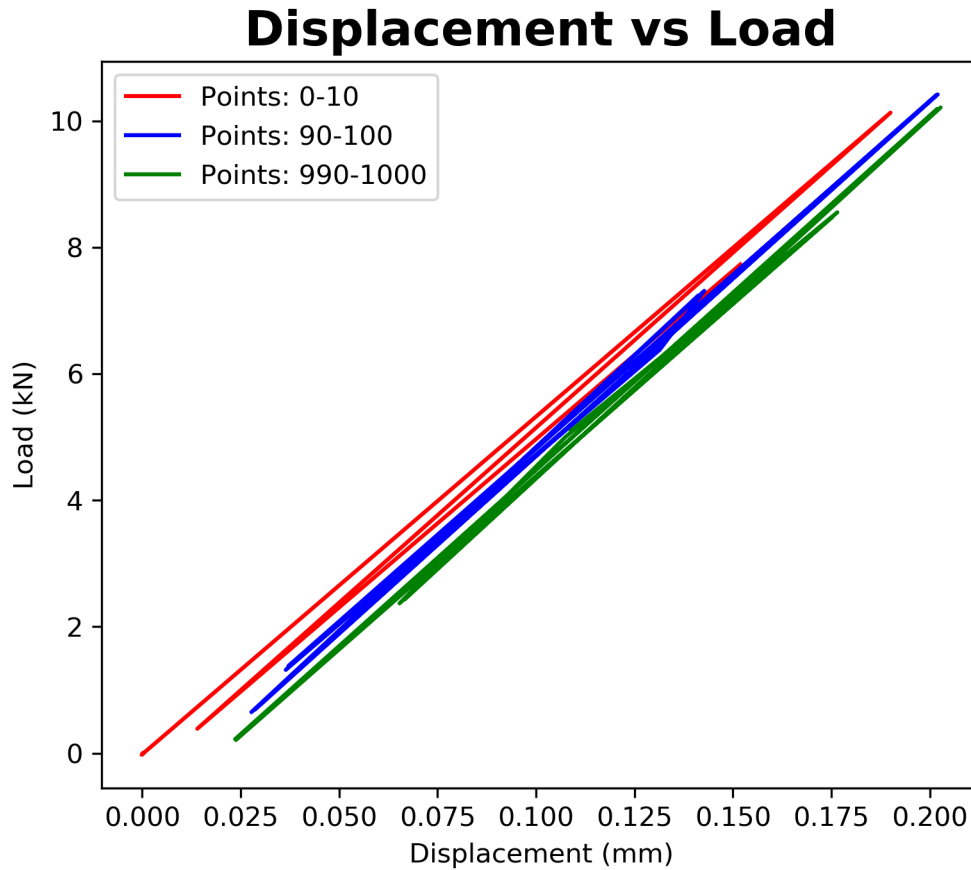


Figure 4.11: Graph displaying point intervals from the displacement vs. load graph for the 90° build oriented test specimen.

The stiffness trend is displayed more clearly in figure 4.11 where the red line represents the interval from points 0 to 10 (the first 10 points in the graph). The blue line represents the interval from points 90 to 100, and lastly the green line represents the interval from points 990 to 1000.

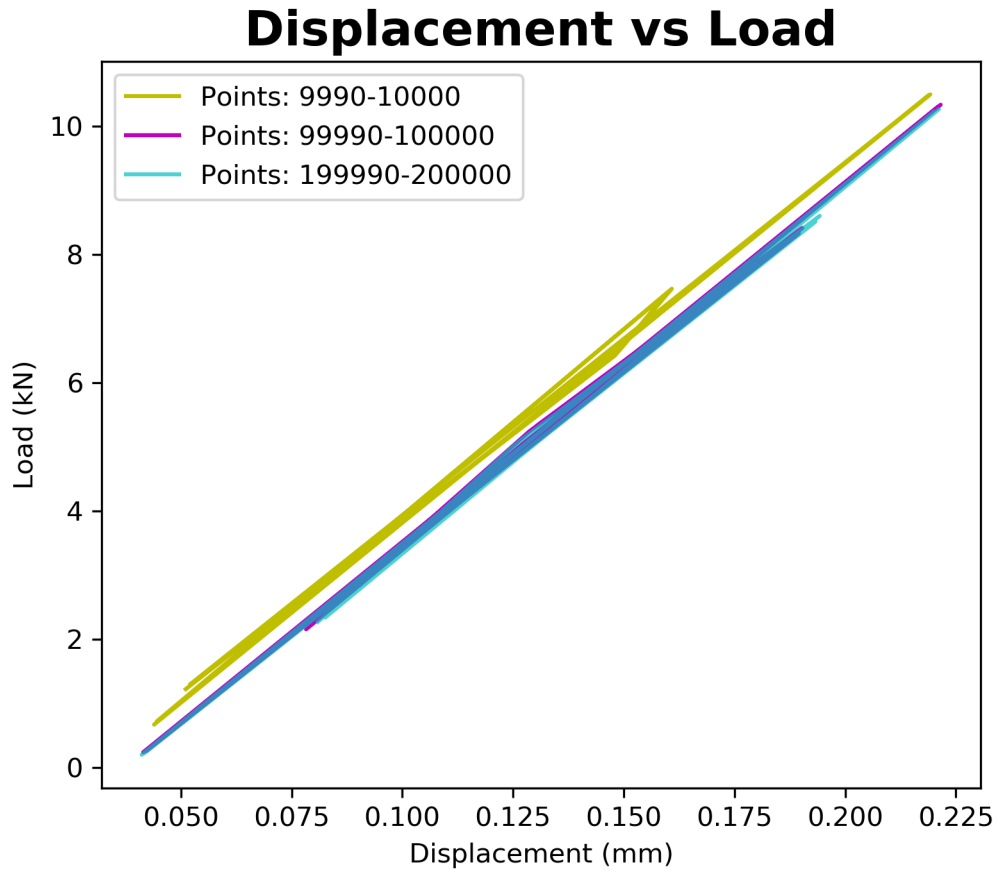


Figure 4.12: Graph displaying point intervals from the displacement vs. load graph for the 90° build oriented test specimen.

The trend is showing a steady progression of higher displacement. However, towards the end of the test, the intervals are staying in the same position as shown in figure 4.12 in interval from points 99,990 to 100,000 and interval from points 199,990 to 200,000.

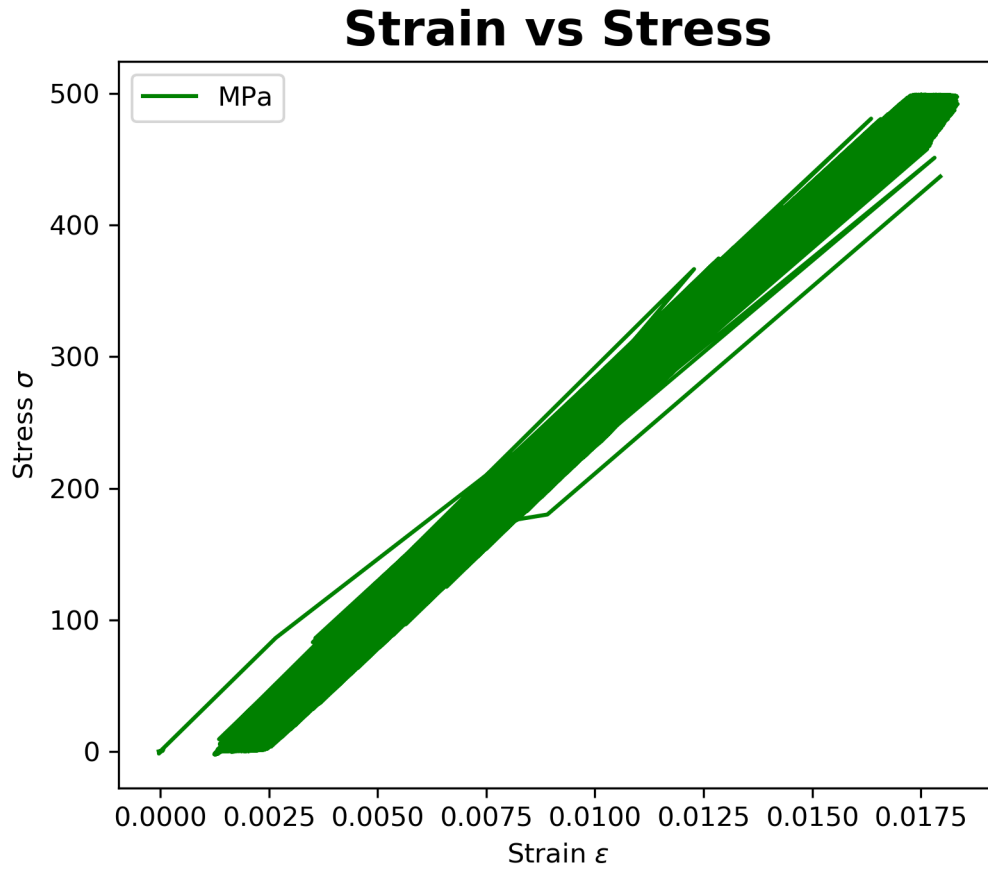


Figure 4.13: Strain vs. stress graph of the 0° build oriented test specimen.

Figure 4.13 shows that for the 0° build oriented specimen the maximum stress is approximately 500 MPa, and that the maximum strain is about 0.0175.

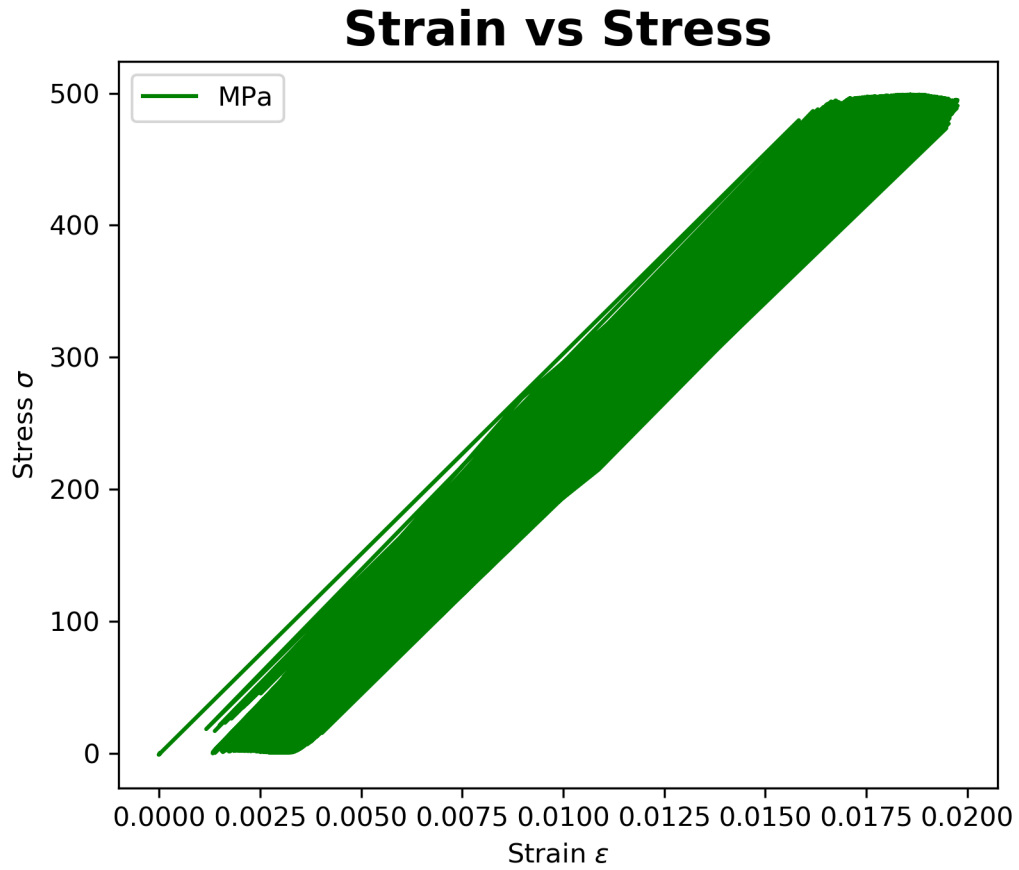


Figure 4.14: Strain vs. stress graph of the 90° build oriented test specimen.

Figure 4.14 shows that for the 90° build oriented specimen the maximum stress is approximately 500 MPa, and that the maximum strain is closing in on about 0.02.

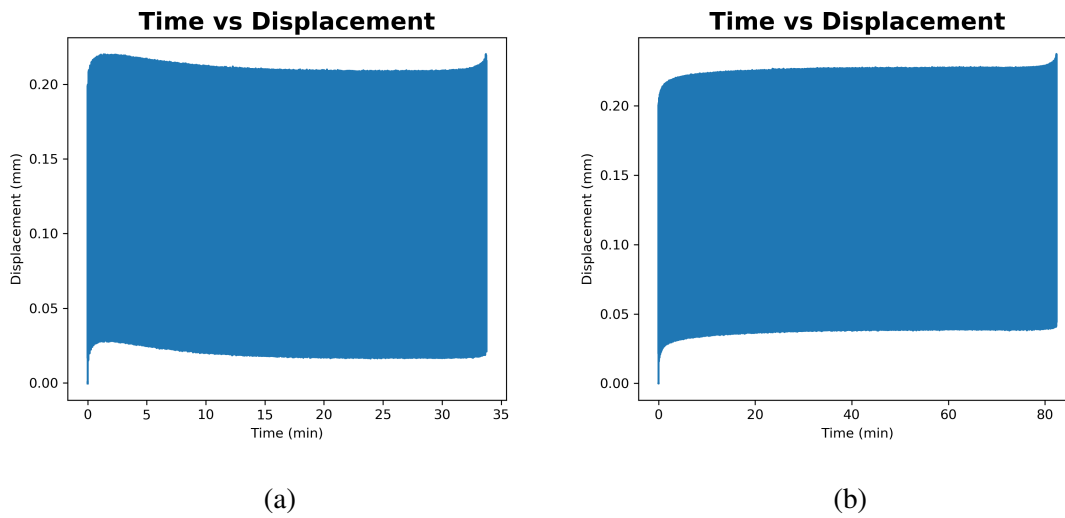


Figure 4.15: Time vs. displacement graphs of the (a) 0° and (b) 90° build oriented specimens.

Figure 4.15 shows that for the 0° build oriented specimen the time until rupture took a little less than 35 minutes, and that the displacement was largest at the beginning and the end of the test. For the 90° build oriented specimen the time until rupture took a little more than 80 minutes, and the displacement was slightly above 0.2 mm with a progressively higher displacement as the test went on.

4.2 S-N Diagrams (Stress-Life Diagrams)

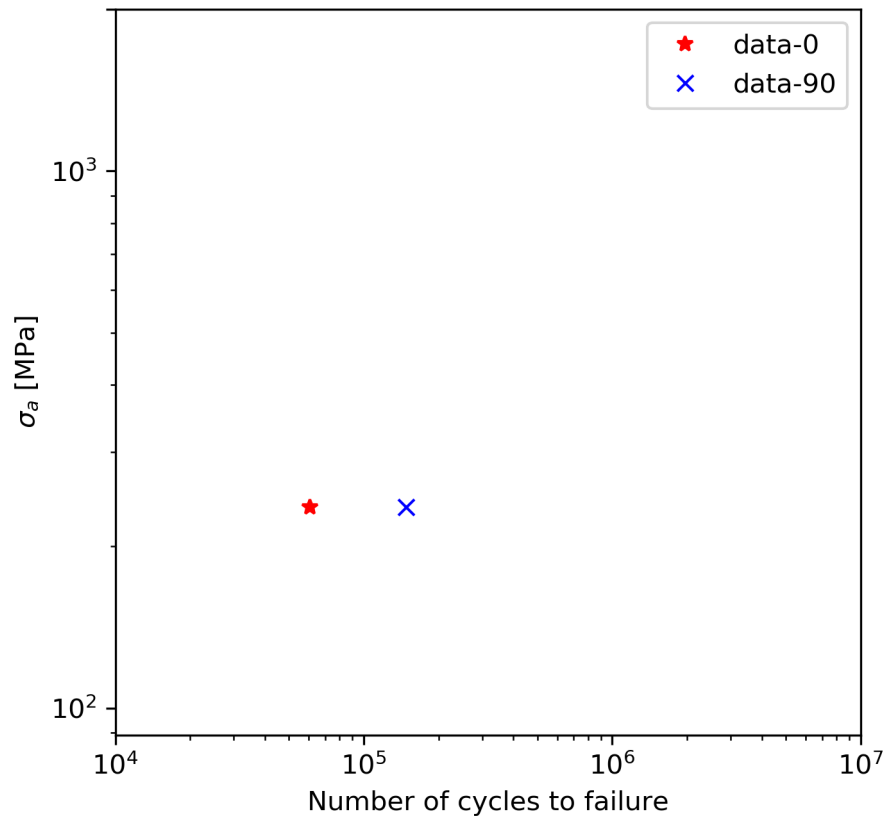


Figure 4.16: Stress amplitude vs. number of cycles to failure.

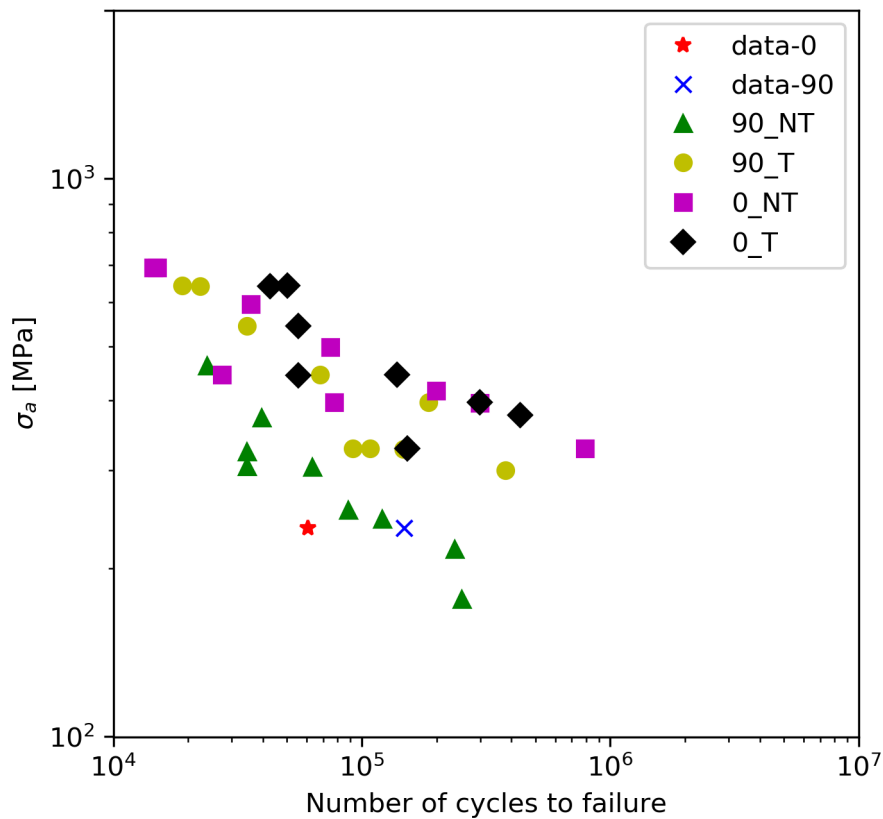


Figure 4.17: Comparison between the stress amplitude vs. number of cycles to failure graph from this study with the study made by Meneghetti et al.¹⁴

Figure 4.16 shows the stress amplitude vs. number of cycles to failure. Both specimens have similar stress amplitude values. A comparison between the results from this study and the study made by Meneghetti et al.¹⁴ is presented in figure 4.17. There are four different specimens from the other study, which include:

- 90° build oriented and not heat treated specimens, denoted as \triangle 90_NT
- 90° build oriented and heat treated specimens, denoted as \circ 90_T
- 0° build oriented and not heat treated specimens, denoted as \square 0_NT
- 0° build oriented and heat treated specimens, denoted as \diamond 0_T

From figure 4.17 it is possible to observe that both 0° and 90° build oriented specimen from this study have similar stress amplitude values and number of cycles to failure as the

90° build oriented and not heat treated specimens (Δ 90_NT).

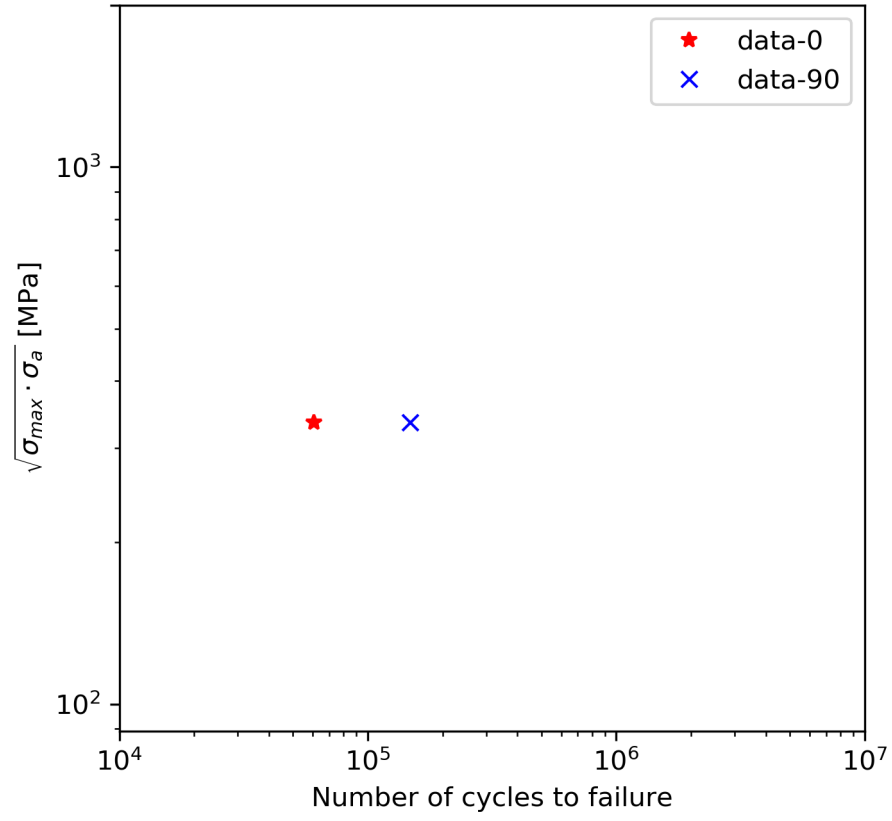


Figure 4.18: SWT parameter vs. number of cycles to failure.

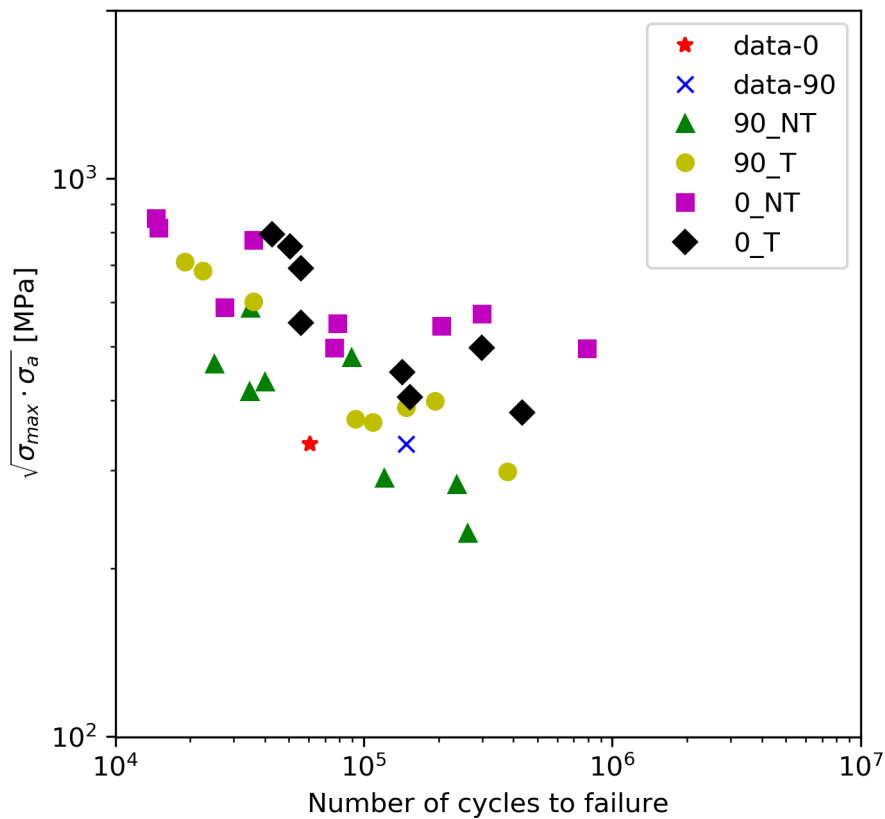


Figure 4.19: Comparison between the SWT parameter vs. number of cycles to failure graph from this study with the study made by Meneghetti et al.¹⁴

Figure 4.18 shows the SWT parameter vs. number of cycles to failure. Both specimens have similar SWT parameter values. A comparison between the results from this study and the study made by Meneghetti et al.¹⁴ is presented in figure 4.19. The specimens from the other study are the same types with the same notations as previously mentioned.

From figure 4.19 it is possible to observe that both 0° and 90° build oriented specimen from this study have similar SWT parameter values and number of cycles to failure as the 90° build oriented and heat treated specimens (\circ 90.T), and slightly similar values as the 90° build oriented and not heat treated specimens (\triangle 90_NT).

4.3 Porosity Results

As mentioned in equation 3.7 in the method chapter about porosity, the percent porosity is measured by dividing the amount of black pixels with the total number of pixels in the image and multiplying it with 100. From the porosity measurement code it counted the number of black and white pixels, as well as the total number of pixels in the image:

Number of black pixels	8600
Number of white pixels	3128936
Total number of pixels	3137536

Table 4.1: Number of black and white pixels, and the total number of pixels.

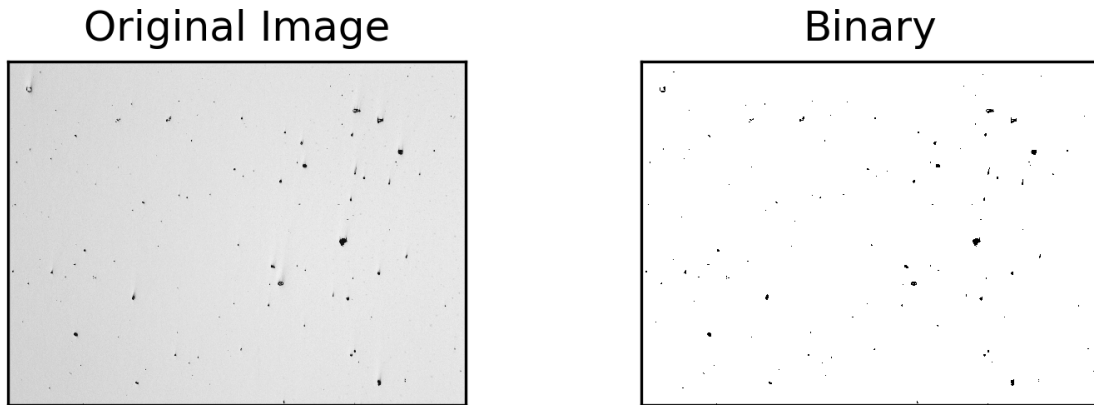


Figure 4.20: Original image compared to the binary image.

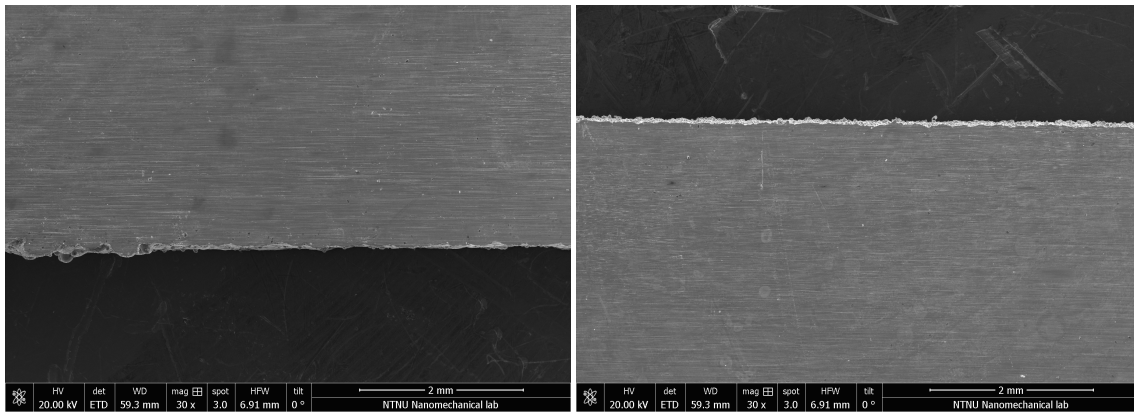
Percent porosity is measured in the following equation:

$$\frac{8600}{3137536} \times 100\% \approx 0.27\% \quad (4.1)$$

The amount of porosity is approximately 0.27%.

4.4 Surface Roughness Results

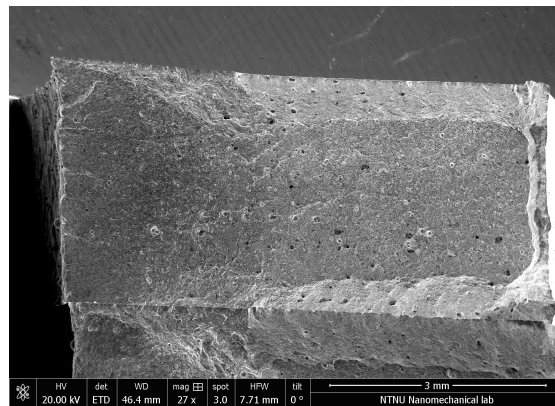
As seen in figure 4.21 the horizontal (0°) build oriented specimen has some areas with bits and particles and overall a more jagged section surface compared to the vertical specimen (90° test specimen).



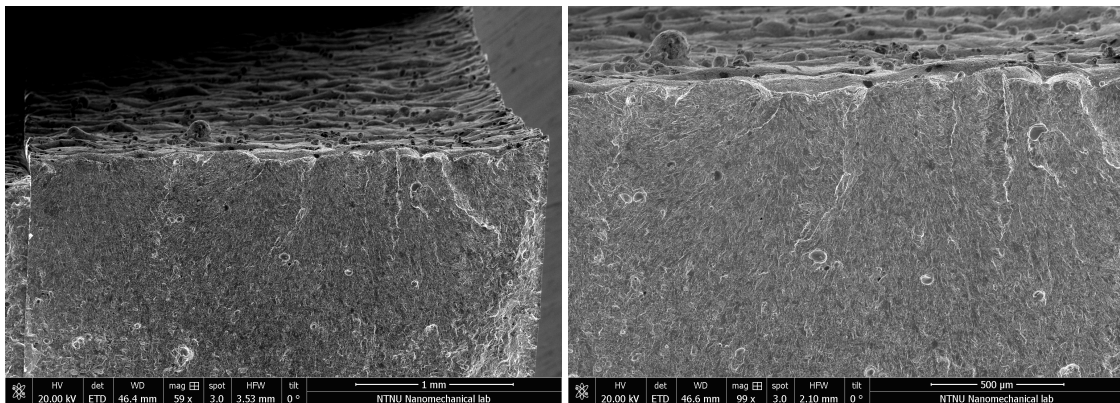
(a)

(b)

Figure 4.21: SEM images of (a) horizontally build oriented specimen section, and (b) vertically build oriented specimen section.



(a)



(b)

(c)

Figure 4.22: SEM images of the fracture surface of the 0° build oriented specimen at (a) 3 mm, (b) 1 mm, and (c) 500 μm .

Figure 4.22 displays the fracture surface of the 0° build oriented specimen. The images display the as-built surface where the surface has a curvy form, and there are bits and particles on the surface, and also a surface defect that is in the shaped of deep valley.

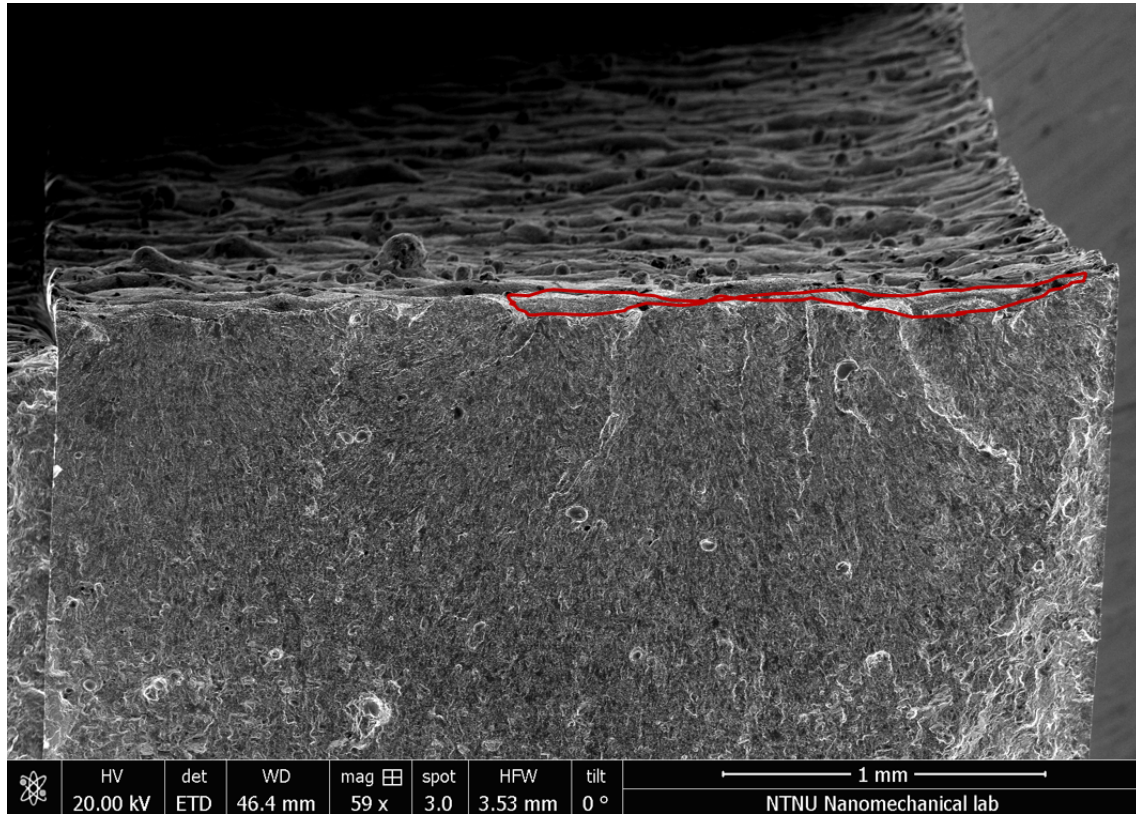


Figure 4.23: The marked surface roughness defect of the 0° build oriented specimen.

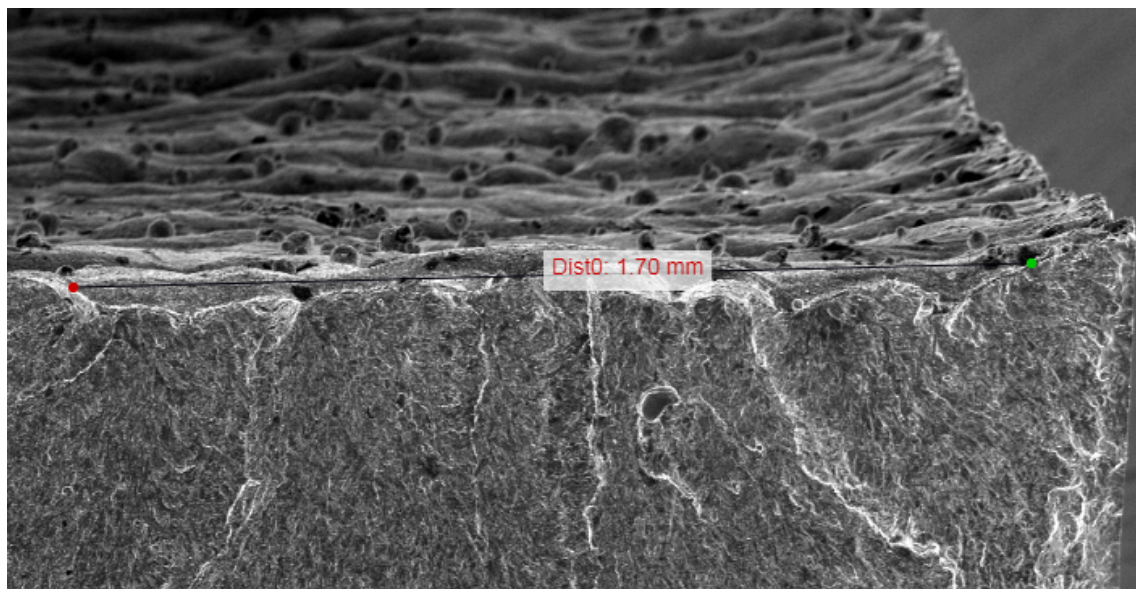
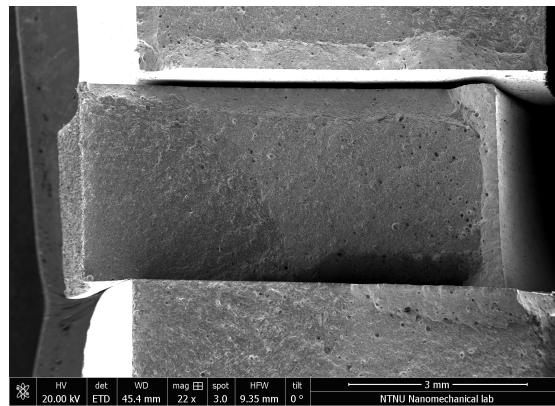
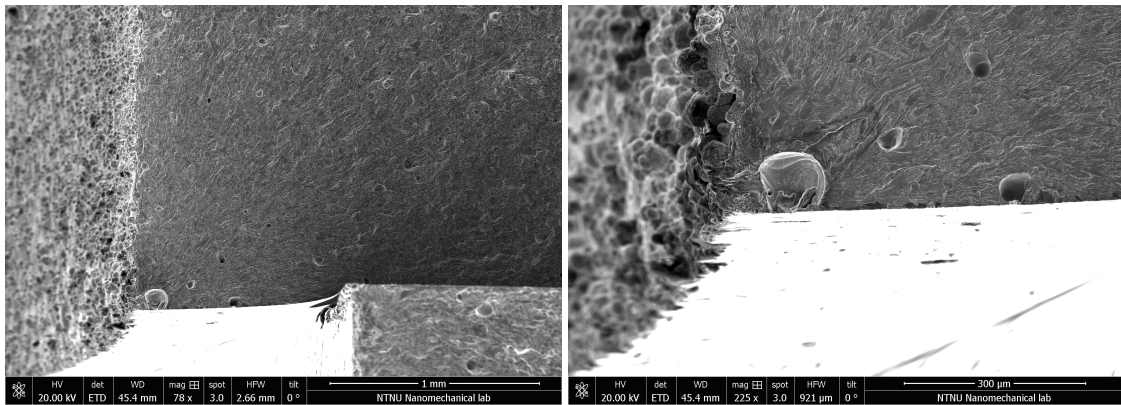


Figure 4.24: A view of defect size measurement of the 0° build oriented specimen.

The valley shaped defect is displayed in figure 4.23. The length of this defect is approximately 1.7 mm, as seen in figure 4.24.



(a)

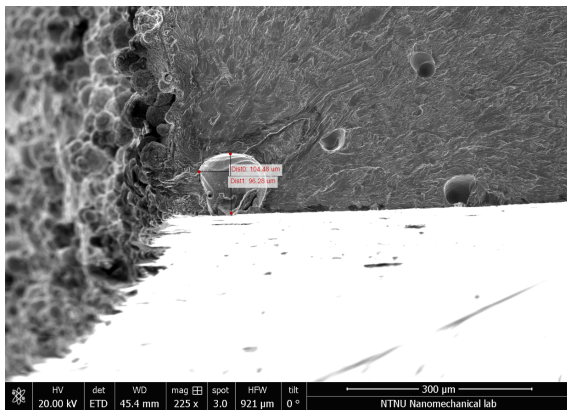


(b)

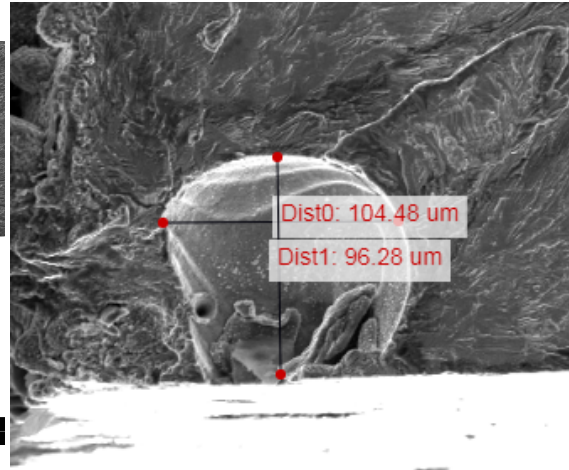
(c)

Figure 4.25: SEM images of the fracture surface of the 90° build oriented specimen at (a) 3 mm, (b) 1 mm, and (c) 300 μm .

Figure 4.25 displays the fracture surface of the 90° build oriented specimen. The images display the as-built surface where the surface has a more even form overall compared to the 0° build oriented specimen, seen in figure 4.22. However, this specimen does have some internal defects on the fracture surface.



(a)



(b)

Figure 4.26: (a) A view of defect size measurement of the 90° build oriented specimen, and (b) magnified view of the defect measurement.

The shape and size of the most noticeable internal defect in the 90° build oriented specimen is a circular shape that is approximately 100 μm in diameter, as seen in figure 4.26.

5 Discussion

In this section, the data from uniaxial ($R = 0$) load controlled fatigue test of two additively manufactured test specimens built in 0° and 90° build orientation has been plotted and studied. Fractography images of surface roughness are obtained from a scanning electron microscope, and porosity images are obtained using an optical microscope. The images are studied, and porosity measurements are compared with the study made by Adriano Fagali de Souza et al.⁷ S-N diagrams are also plotted in order to compare the results from this study with the study made by Meneghetti et al.¹⁴ The surface roughness is observed in order to get a clearer view of how many irregularities, pores and other abnormalities there are on the test specimen, and to observe the effect of surface roughness on the test specimens.

5.1 Analysis of the Graphs

From observing the graphs it is clear that the 90° build oriented (vertical) test specimen lasted over double the amount of cycles than the 0° build oriented (horizontal) test specimen. The 90° build oriented specimen had over 140,000 cycles before fracture occurred, while the 0° build oriented specimen had over 60,000 cycles. The result that the vertically built specimen lasts longer than the horizontally built specimen is in contrast with the study made by Yadollahi et al.³⁰ which found that horizontally built AM 17-4 precipitation hardened stainless steel specimen had a higher elongation to failure compared to the vertically built specimen. This is because vertically built specimens have deposited layers that are perpendicular to the loading axis, meaning that the defects between the layers are also perpendicular to the loading axis leading to a much higher stress concentration compared to the horizontally built specimens, which makes the vertical specimen more prone to openings and crack initiations. The horizontally built specimens however, have deposited layers and thus defects between the layers, that are parallel to the loading axis leading to a lower stress concentration than the vertically built specimen.³⁰

Possible explanations for the vertically built specimen lasting longer than the horizontally built specimen can be found in the study by Qiu et al.²¹ which found that the vertically built specimen made of Ti-6Al-4V had better ductility than the horizontally built specimens, mainly due to the orientation of the columnar grains with respect to the loading axis. It was also found that the vertical specimen had lower amount of porosity compared

to the horizontal specimen, which was discussed that this may be due to the different thermal history.²¹

The maximum displacement and stiffness are relatively similar for both test specimens. Maximum displacement was little over 0.2 mm, while the maximum stiffness was approximately $50 \frac{kN}{mm}$ throughout the entire tests with the exception during the beginning of the tests where the stiffness had large spikes, which are caused by the load being divided with displacement values close to zero. The maximum load and stress are also similar for both specimens, with the maximum load being roughly 10 kN and the maximum stress being close to 500 MPa.

A trend in stiffness was observed by dividing the displacement vs. load graph into intervals of 10 points as seen in figure 4.8 and 4.11. One interval had the points 0 to 10 (the first 10 points in the graph), another interval had the points 90 to 100, and so on. The trend was that the stiffness was consistent/stable throughout the whole test and the displacement became gradually larger. The exception for the 0° specimen is at the end of the test where the last interval goes behind the previous interval as seen in figure 4.9. For the 90° specimen, the last intervals stayed in one place as seen in figure 4.12. The reason for these exceptions might be because of how the fatigue test machine was calibrated.

5.2 S-N Diagrams

As mentioned previously, the 90° build oriented (vertical) test specimen has more cycles until failure than the 0° build oriented (horizontal) test specimen, while the stress amplitude values and SWT parameter values for both specimens are identical. Both the 0° and 90° build oriented test specimen have a stress amplitude that is roughly 250 MPa, and a SWT parameter value that is above 300 MPa. The stress amplitude values and the number of cycles to failure for both 0° and 90° build oriented specimens from this study are similar to the 90° build oriented not heat treated specimens, as seen in figure 4.17. The SWT parameter values and the number of cycles to failure for both 0° and 90° build oriented specimens from this study are most similar to the 90° build oriented heat treated specimens, but also slightly similar to the 90° build oriented not heat treated specimens, as seen in figure 4.19.

5.3 Analysis of the Porosity

The percent porosity was measured on the 90° build oriented (vertical) specimen and it was approximately 0.27%. Porosity was measured by obtaining the number of black pixels and the total number of pixels through coding, and thus dividing the black pixels with the total number of pixels and multiplying it with 100. This value is befitting the values found in the study by Adriano Fagali de Souza et al..⁷

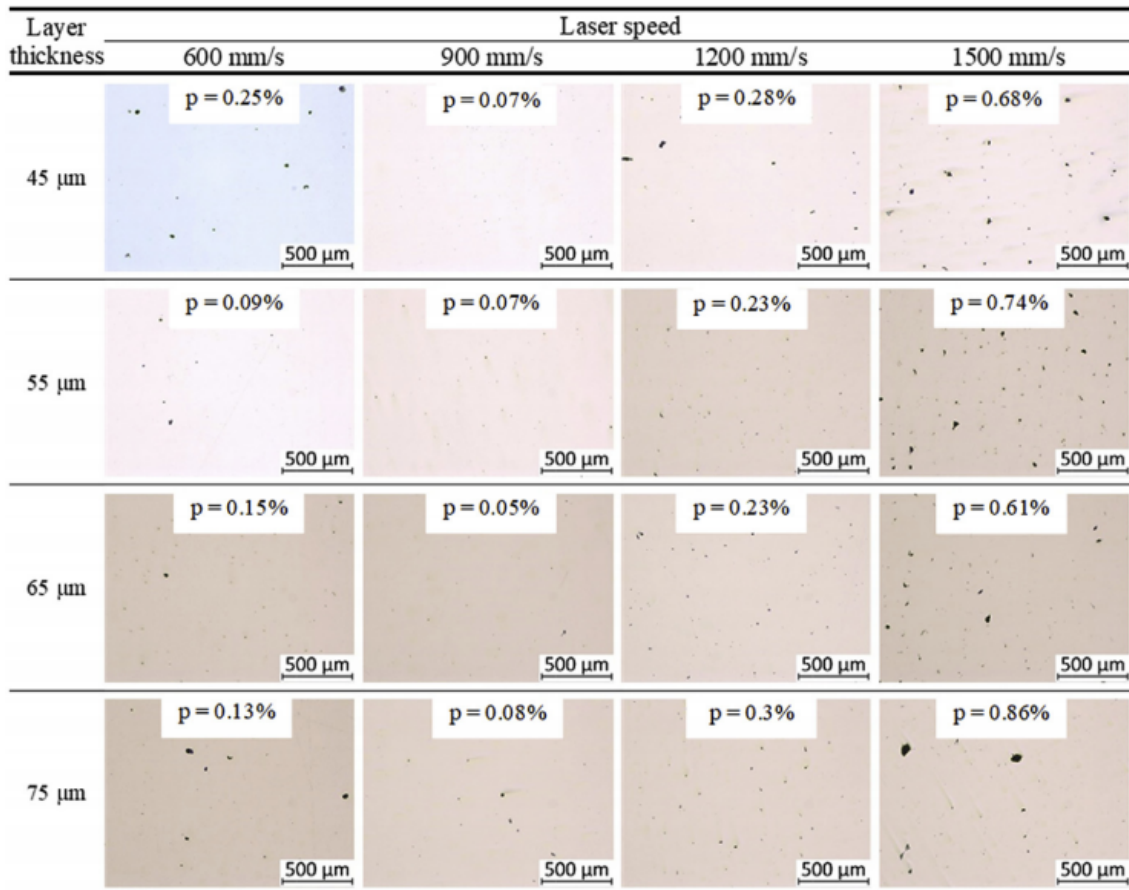


Figure 5.1: Porosity measurements from the article by Adriano Fagali de Souza et al..⁷

The study made by Adriano Fagali de Souza et al..⁷ inspected the effect of laser speed, layer thickness and part position on the mechanical properties of AM Maraging 300 steels. One of the studies was on the effect of laser speed and layer thickness on the porosity of the parts. Test specimens from this study are made with a scanning velocity of 650 $\frac{\text{mm}}{\text{s}}$ and layer thickness of 30 μm . The percent porosity found in this study, 0.27%, is closest to the 0.28% porosity, which is found when laser speed is 1200 $\frac{\text{mm}}{\text{s}}$ and layer thickness is 45 μm , as seen in figure 5.1. It is also close to the 0.25% porosity which is found when

laser speed is $600 \frac{mm}{s}$ and layer thickness is $45 \mu m$.

5.4 Analysis of the Surface Roughness

Surface roughness is displayed through SEM images which displays the fracture surface, the surface that underwent machining, and the as-built surface, a surface that underwent no forms of after treatment. The reason for the as-built surface was to see the effect of surface roughness. As seen in the figures 4.21, 4.22, and 4.25 it appears that the 90° build oriented specimen has a more even surface compared to the 0° build oriented specimen, which has a wavy surface form with bits or particles attached to the surface. The apparently rougher surface of the 0° build oriented specimen might be caused by the staircase effect, where during printing the deposited layers are forming stair-step formation due to the curvature of the surface and the layer thickness.¹³ This jagged surface form might be a reason to why the 0° build oriented (horizontal) specimen did not last longer than the 90° build oriented (vertical) specimen, even though the article by Yadollahi et al.³⁰ discusses that the horizontally built specimens last longer than the vertically built specimens.

From observing the fracture surface images displayed in figure 4.25 it can be discussed that for the 90° build oriented specimen the fracture initiates from an internal defect and not from the surface roughness. For the 0° build oriented specimen however, it is possible to observe from figure 4.22, 4.23, and 4.24 that the fracture initiated from the surface roughness and that the defect has a deep valley shape with a length of roughly 1.7 mm. The internal defect of the 90° build oriented specimen has a slightly circular shape with a diameter of roughly $100 \mu m$, which is reasonably large for a defect. Comparing the size and shape of the defect with the defects presented in the article by Molaei et al.¹⁵ and the article by Yadollahi et al.³⁰ leads to the assumption that this defect is a void that is caused by lack of fusion (LOF) as it is too large to be a regular pore. In addition, the defect is located near the surface of the specimen, and according to Yadollahi et al.,³⁰ defects that are located close to the surface are the most detrimental as they have the shortest distance to the surface and can cause accelerating crack growth rate that ultimately leads to failure.³⁰

Despite the relatively large internal defect of the 90° (vertical) build oriented specimen, and its deposited layers that are perpendicular to the loading axis, it is still the specimen that lasts the longest, which can show how much of an influence the surface roughness can have on an AM component. If the internal defect did not exist in the specimen, it would be reasonable to assume that the specimen would have lasted even longer.

6 Conclusion

In this study, data from uniaxial fatigue test performed on two additively manufactured test specimens made of Maraging 300 steel with each of the specimens having one as-built surface are analysed by plotting graphs and S-N diagrams, and compared with existing studies. Percent porosity is measured on one of the specimens and the result is compared with existing studies. Lastly, SEM images of fracture surfaces and surface roughness for both specimens are investigated and analysed.

The data for the uniaxial ($R = 0$) load controlled fatigue test has been obtained for horizontally (0°) and vertically (90°) build oriented test specimens. Plotting the data shows that the 90° build oriented (vertical) test specimen lasts over twice as long as the 0° build oriented (horizontal) test specimen. This result that the vertical specimen outlasts the horizontal specimen is in contrast with the study made by Yadollahi et al.³⁰ which found that the horizontally built specimen have a higher elongation to failure compared to the vertically built specimen. This elongation is attributed to defects between layers in the vertical specimen being perpendicular to the loading axis, giving a much higher stress concentration compared to the defects between layers in the horizontally built specimen that are parallel to the loading axis.³⁰ The lower amount of cycles in the horizontally built specimen is most likely caused by the rough surface of the specimen. However, the vertically build oriented specimen had a reasonably large internal defect, that was probably a lack of fusion (LOF) void, close to the surface. It is reasonable to assume this defect decreased the amount of cycles the specimen otherwise could have lasted. This shows that surface roughness has a major influence on the AM components.

The graphs show that the maximum displacement and maximum stiffness for both tests are approximately 0.2 mm and $50 \frac{kN}{mm}$ respectively. The graphs also show that the maximum load and maximum stress for both tests are approximately 10 kN and 500 MPa respectively.

Results from the S-N diagrams show that the stress amplitude for both specimens are close to 250 MPa. Compared with the study made by Meneghetti et al.,¹⁴ the two test specimens from this study have a similar stress amplitude value and number of cycles to failure as the 90° build oriented not heat treated specimens. The SWT parameter values for both test specimen are above 300 MPa. Compared with the study made by Meneghetti et al.,¹⁴ both specimens from this study have a similar SWT parameter value and number

of cycles to failure as the 90° build oriented heat treated specimens, and have slightly similar values as the 90° build oriented not heat treated specimens.

Porosity measurements show that the percent porosity is approximately 0.27% for the vertically (90°) built specimen. Another study made by Adriano Fagali de Souza et al.,⁷ measured the percent porosity and studied the effect of laser speed and layer thickness on the porosity. Comparing the porosity measurement from this study with the one made by Adriano Fagali de Souza et al.,⁷ shows that the percent porosity from this study is close to 0.28% porosity and 0.25% porosity. The specimen from this study was made with layer thickness of 30 μm and scan velocity of 650 mm/s, while the 0.28% porosity was the result of the laser speed being 1200 $\frac{mm}{s}$ and the layer thickness being 45 μm . While the 0.25% porosity was the result of the laser speed being 600 $\frac{mm}{s}$ and the layer thickness being 45 μm .

SEM images of the surface roughness show that the horizontally (0°) built specimen has a overall rougher surface on the as-built side compared to the vertically (90°) built specimen, which might be caused by the staircase effect. The horizontally built specimen fracture initiates from the surface roughness, where a deep valley shaped defect with a length of approximately 1.7 mm is present. While for the vertically built specimen fracture initiates from an internal defect, which is circular shaped with roughly 100 μm in diameter that is most likely a lack of fusion (LOF) void located close to the surface.

Bibliography

- [1] <https://automeris.io/WebPlotDigitizer/>.
- [2] <https://jupyter.org/>.
- [3] <https://pandas.pydata.org/>.
- [4] <https://matplotlib.org/>.
- [5] <https://numpy.org/>.
- [6] F Baumgart. Stiffness-an unknown world of mechanical science? *Injury-International Journal for the Care of the Injured*, 31(2):14–23, 2000.
- [7] Adriano Fagali de Souza, Kassim S Al-Rubaie, Sabrina Marques, Bruno Zluhan, and Edson Costa Santos. Effect of laser speed, layer thickness, and part position on the mechanical properties of maraging 300 parts manufactured by selective laser melting. *Materials Science and Engineering: A*, 767:138425, 2019.
- [8] William E Frazier. Metal additive manufacturing: a review. *Journal of Materials Engineering and Performance*, 23(6):1917–1928, 2014.
- [9] Nannan Guo and Ming C Leu. Additive manufacturing: technology, applications and research needs. *Frontiers of Mechanical Engineering*, 8(3):215–243, 2013.
- [10] International Molybdenum Association (IMOA). Maraging steel. Available at: <https://www.imoa.info/molybdenum-uses/molybdenum-grade-alloy-steels-irons/maraging-steels.php>.
- [11] Karolien Kempen, Evren Yasa, Lore Thijs, J-P Kruth, and Jan Van Humbeeck. Microstructure and mechanical properties of selective laser melted 18ni-300 steel. *Physics Procedia*, 12:255–263, 2011.
- [12] Daniel Kujawski. A deviatoric version of the swt parameter. *International journal of fatigue*, 67:95–102, 2014.
- [13] P Li, DH Warner, A Fatemi, and N Phan. Critical assessment of the fatigue performance of additively manufactured ti–6al–4v and perspective for future research. *International Journal of Fatigue*, 85:130–143, 2016.

- [14] G Meneghetti, D Rigon, D Cozzi, W Waldhauser, and M Dabalà. Influence of build orientation on static and axial fatigue properties of maraging steel specimens produced by additive manufacturing. *Procedia Structural Integrity*, 7:149–157, 2017.
- [15] Reza Molaei and Ali Fatemi. Fatigue design with additive manufactured metals: issues to consider and perspective for future research. *Procedia engineering*, 213:5–16, 2018.
- [16] Nestor Perez. The energy principle. In *Fracture Mechanics*, pages 227–256. Springer International Publishing, Cham, 2017.
- [17] Nestor Perez. Fatigue crack growth. In *Fracture Mechanics*, pages 327–372. Springer International Publishing, Cham, 2017.
- [18] Nestor Perez. Introduction to fracture mechanics. In *Fracture Mechanics*, pages 53–77. Springer International Publishing, Cham, 2017.
- [19] Nestor Perez. Theory of elasticity. In *Fracture Mechanics*, pages 1–52. Springer International Publishing, Cham, 2017.
- [20] P Ponnusamy, SH Masood, S Palanisamy, RA Rahman Rashid, and D Ruan. Characterization of 17-4ph alloy processed by selective laser melting. *Materials Today: Proceedings*, 4(8):8498–8506, 2017.
- [21] Chunlei Qiu, Nicholas JE Adkins, and Moataz M Attallah. Microstructure and tensile properties of selectively laser-melted and of hiped laser-melted ti-6al-4v. *Materials Science and Engineering: A*, 578:230–239, 2013.
- [22] NS Rossini, Michele Dassisti, KY Benyounis, and Abdul-Ghani Olabi. Methods of measuring residual stresses in components. *Materials & Design*, 35:572–588, 2012.
- [23] Nima Shamsaei and Jutima Simsiriwong. Fatigue behaviour of additively-manufactured metallic parts. *Procedia Structural Integrity*, 7:3–10, 2017.
- [24] K.N. Smith, Tim Topper, and P. Watson. A stress–strain function for the fatigue of metals (stress-strain function for metal fatigue including mean stress effect). *J Materials*, 5:767–778, 01 1970.
- [25] K Solberg, J Torgersen, and F Berto. Fatigue behaviour of additively manufactured inconel 718 produced by selective laser melting. *Procedia Structural Integrity*, 13:1762–1767, 2018.

- [26] Klas Solberg and Filippo Berto. Notch-defect interaction in additively manufactured inconel 718. *International Journal of Fatigue*, 122:35–45, 2019.
- [27] Klas Solberg and Filippo Berto. What is going on with fatigue of additively manufactured metals? *Material Design & Processing Communications*, 1(5):e84, 2019.
- [28] Klas Solberg, Shuai Guan, Seyed Mohammad Javad Razavi, Torgeir Welo, Kang Cheung Chan, and Filippo Berto. Fatigue of additively manufactured 316l stainless steel: The influence of porosity and surface roughness. *Fatigue & Fracture of Engineering Materials & Structures*, 42(9):2043–2052, 2019.
- [29] EG Thorsteinsdóttir, DS Primdahl, YB Zhang, D Juul Jensen, and T Yu. Aging of 3d-printed maraging steel. In *IOP Conference Series: Materials Science and Engineering*, volume 580, page 012047. IOP Publishing, 2019.
- [30] Aref Yadollahi, Nima Shamsaei, Scott M Thompson, Alaa Elwany, and Linkan Bian. Effects of building orientation and heat treatment on fatigue behavior of selective laser melted 17-4 ph stainless steel. *International Journal of Fatigue*, 94:218–235, 2017.

A Coding

```
1 import matplotlib.pyplot as plt
2 import numpy as np
3 import pandas as pd
4
5 data = pd.read_csv('data-0.csv', sep=";")
6
7 plt.figure(figsize=(5.9,5))
8
9 plt.title('Cycles vs Displacement', fontdict={'fontweight':'bold', '
    fontsize': 18})
10
11 plt.plot(data.cycles, data.mm, '-')
12
13 plt.xlabel('Cycles')
14 plt.ylabel('Displacement')
15
16 plt.legend()
17
18 #Limiting the axis, showig e.g. values from 0 to 100. gca = Get the
    Current Axis
19 ax = plt.gca()
20 # ax.set_xlim([0,20])
21 ax.set_ylim([0,0.4])
22
23 plt.savefig('Cycles_vs_displacement_0.png', dpi=300)
24
25 plt.show()
```

Listing A.1: Complete code for the cycles vs. displacement graph.

```
1 import matplotlib.pyplot as plt
2 import numpy as np
3 import pandas as pd
4
5 data = pd.read_csv('data-0.csv', sep=";")
6
7 plt.figure(figsize=(5.9,5))
8
9 plt.title('Cycles vs Stiffness', fontdict={'fontweight':'bold', '
    fontsize': 18})
```

```

10
11 stiffness = (data.kN/data.mm)
12
13 plt.plot(data.cycles, stiffness, 'b-', label='kN/mm')
14
15 plt.xlabel('Cycles')
16 plt.ylabel('Stiffness')
17
18 plt.legend()
19
20 ax = plt.gca()
21 ax.set_xlim([59900,60000])
22 ax.set_ylim([0,70])
23
24 #plt.savefig('Cycles_vs_stiffness_0.png', dpi=300)
25
26 plt.show()

```

Listing A.2: Complete code for the cycles vs. stiffness graph.

```

1 import matplotlib.pyplot as plt
2 import numpy as np
3 import pandas as pd
4
5 data = pd.read_csv('data-0.csv', sep=";")
6
7 stiffness = (data.kN/data.mm)
8
9 plt.figure(figsize=(5.9,5))
10
11 plt.title('The upper part of the cycles vs stiffness curve', fontdict={
12     'fontweight': 'bold', 'fontsize': 14})
13
14 maxVal = 51
15 stiffness[stiffness < maxVal] = maxVal
16
17 plt.plot(data.cycles, stiffness, '- ', label='kN/mm')
18
19 plt.xlabel('Cycles')
20 plt.ylabel('Stiffness')
21
22 plt.legend()
23
24 plt.savefig('Cycles_vs_stiffness_upper_0.png', dpi=300)

```

```
24
25 plt.show()
```

Listing A.3: Complete code for obtaining the upper part of the cycles vs. stiffness graph.

```
1 import matplotlib.pyplot as plt
2 import numpy as np
3 import pandas as pd
4
5 data = pd.read_csv('data-0.csv', sep=";")
6
7 stiffness = (data.kN/data.mm)
8
9 plt.figure(figsize=(5.9,5))
10
11 maxVal = 51
12 stiffness[stiffness < maxVal] = maxVal
13
14 stiffness_norm = (data.kN/data.mm)
15 cycles = data.cycles
16
17 plt.plot(data.cycles, stiffness, 'y-', linewidth=3, label='kN/mm')
18 plt.plot(cycles, stiffness_norm, '-', label='kN/mm', alpha=0.5)
19
20 plt.xlabel('Cycles')
21 plt.ylabel('Stiffness [kN/mm]')
22 plt.show()
```

Listing A.4: Complete code for displaying the upper part and the normal cycles vs. stiffness graph together.

```
1 import matplotlib.pyplot as plt
2 import numpy as np
3 import pandas as pd
4
5 data = pd.read_csv('data-0.csv', sep=";")
6
7 plt.figure(figsize=(5.9,5))
8
9 plt.title('Displacement vs Stress', fontdict={'fontweight':'bold', '
    fontsize': 18})
10
11 area = 6.5*3.25
12 stress = (data.kN/area)*1000
```

```

13
14 plt.plot(data.mm[:-8], stress[:-8], '-', label="MPa")
15
16 plt.xlabel('Displacement (mm)')
17 plt.ylabel('Stress  $\sigma$ ')
18 plt.legend()
19
20 plt.rcParams['agg.path.chunksize'] = 10000
21
22 plt.savefig('Displacement_vs_stress_0.png', dpi=300)
23
24 plt.show()

```

Listing A.5: Complete code for the displacement vs. stress graph.

```

1 import matplotlib.pyplot as plt
2 import numpy as np
3 import pandas as pd
4
5 data = pd.read_csv('data-0.csv', sep=";")
6
7 plt.figure(figsize=(5.9,5))
8
9 plt.title('Displacement vs Load', fontdict={'fontweight':'bold', '
    fontsize': 18})
10
11 plt.plot(data.mm[:-8], data.kN[:-8], 'r-', label='kN')
12
13 plt.xlabel('Displacement (mm)')
14 plt.ylabel('Load')
15
16 plt.legend()
17
18 plt.savefig('Displacement_vs_load_0.png', dpi=300)
19
20 plt.show()

```

Listing A.6: Complete code for the displacement vs. load graph.

```

1 import matplotlib.pyplot as plt
2 import numpy as np
3 import pandas as pd
4
5 data = pd.read_csv('data-0.csv', sep=";")

```

```

6
7 plt.figure(figsize=(5.9,5))
8
9 plt.title('Strain vs Stress', fontdict={'fontweight':'bold', 'fontsize'
: 18})
10
11 area = 6.5*3.25
12 stress = (data.kN/area)*1000
13 strain = ((12+data.mm)-12)/(12)
14
15 plt.plot(strain[:-8], stress[:-8], 'g-', label='MPa')
16
17 plt.xlabel('Strain  $\epsilon$ ')
18 plt.ylabel('Stress  $\sigma$ ')
19 plt.legend()
20
21 plt.rcParams['agg.path.chunksize'] = 10000
22 #Fixes overflowerror
23
24 plt.savefig('Stress_vs_strain_0.png', dpi=300)
25
26 plt.show()

```

Listing A.7: Complete code for the stress vs. strain graph.

```

1 import matplotlib.pyplot as plt
2 import numpy as np
3 import pandas as pd
4
5 data = pd.read_csv('data-0.csv', sep=";")
6
7 plt.figure(figsize=(5.9,5))
8
9 plt.title('Time vs Displacement', fontdict={'fontweight':'bold', '
fontsize': 18})
10
11 minutes = data.sec/60
12
13 plt.plot(minutes[:-8], data.mm[:-8], '-')
14
15 plt.xlabel('Time (min)')
16 plt.ylabel('Displacement (mm)')
17
18 plt.savefig('Time_vs_displacement_0.png', dpi=300)

```

```
19
20 plt.show()
```

Listing A.8: Complete code for the time vs. displacement graph.

```
1 import matplotlib.pyplot as plt
2 import numpy as np
3 import pandas as pd
4
5 data_0 = pd.read_csv('data-0.csv', sep=";")
6 data_90 = pd.read_csv('data-90.csv', sep=";")
7
8 plt.figure(figsize=(5,5))
9
10 area = 6.5*3.25
11 stress_0 = (data_0.kN/area)*1000
12 stress_90 = (data_90.kN/area)*1000
13
14 ymax = 10000/(area)
15 ymin = 0/(area)
16
17 # Cycles for 0 and 90 specimen
18 x_xmax = data_0.cycles[np.argmax(data_0.cycles)]
19 x_xmax_90 = data_90.cycles[np.argmax(data_90.cycles)]
20
21 S_0 = (ymax-ymin)/2
22 N_0 = 60760
23
24 S_90 = (ymax-ymin)/2
25 N_90 = 148339
26
27 plt.loglog(N_0, S_0, 'r*', label='data-0')
28 plt.loglog(N_90, S_90, 'bx', label='data-90')
29
30 plt.xlabel('Number of cycles to failure')
31 plt.ylabel('$\sigma_a$ [MPa]')
32 plt.legend()
33
34 plt.xticks([1E+4, 1E+5, 1E+6, 1E+7])
35 plt.yticks([100, 1000, 2000])
36
37 plt.savefig('stress_amp_vs_cycles.png', dpi=300)
38
```

```
39 plt.show()
```

Listing A.9: Complete code for S-N diagram with stress amplitude vs. number of cycles to failure as parameters.

```
1 import matplotlib.pyplot as plt
2 import numpy as np
3 import pandas as pd
4
5 data_0 = pd.read_csv('data-0.csv', sep=";")
6 data_90 = pd.read_csv('data-90.csv', sep=";")
7
8 AD0NT = pd.read_csv('AD0NT.csv', sep=";")
9 AD0T = pd.read_csv('AD0T.csv', sep=";")
10 AD90NT = pd.read_csv('AD90NT.csv', sep=";")
11 AD90T = pd.read_csv('AD90T.csv', sep=";")
12
13 plt.figure(figsize=(5,5))
14
15 area = 6.5*3.25
16 stress_0 = (data_0.kN/area)*1000
17 stress_90 = (data_90.kN/area)*1000
18
19 ymax = 10000/(area)
20 ymin = 0/(area)
21
22 # Cycles for 0 and 90 specimen
23 x_xmax = data_0.cycles[np.argmax(data_0.cycles)]
24 x_xmax_90 = data_90.cycles[np.argmax(data_90.cycles)]
25
26 S_0 = (ymax-ymin)/2
27 N_0 = 60760
28
29 S_90 = (ymax-ymin)/2
30 N_90 = 148339
31
32 plt.loglog(N_0, S_0, 'r*', label='data-0')
33 plt.loglog(N_90, S_90, 'bx', label='data-90')
34
35 plt.loglog(AD0NT.X, AD0NT.Y, 'g^', label='90_NT')
36 plt.loglog(AD0T.X, AD0T.Y, 'yo', label='90_T')
37 plt.loglog(AD90NT.X, AD90NT.Y, 'ms', label='0_NT')
38 plt.loglog(AD90T.X, AD90T.Y, 'kD', label='0_T')
39
```



```

40 plt.xlabel('Number of cycles to failure')
41 plt.ylabel('\sigma_a$ [MPa]')
42 plt.legend()
43
44 plt.xticks([1E+4, 1E+5, 1E+6, 1E+7])
45 plt.yticks([100, 1000, 2000])
46
47 plt.savefig('stress_amp_vs_cycles_merged.png', dpi=300)
48
49 plt.show()

```

Listing A.10: Complete code for comparing stress amplitude vs. number of cycles to failure graph between this study and existing studies.

```

1 import matplotlib.pyplot as plt
2 import numpy as np
3 import pandas as pd
4 import math
5
6 data_0 = pd.read_csv('data-0.csv', sep=";")
7 data_90 = pd.read_csv('data-90.csv', sep=";")
8
9 plt.figure(figsize=(5,5))
10
11 area = 6.5*3.25
12 stress_0 = (data_0.kN/area)*1000
13 stress_90 = (data_90.kN/area)*1000
14
15 ymax = 10000/(area)
16 ymin = 0/(area)
17
18 # Cycles for 0 and 90 specimen
19 x_xmax = data_0.cycles[np.argmax(data_0.cycles)]
20 x_xmax_90 = data_90.cycles[np.argmax(data_90.cycles)]
21
22 S_0 = (ymax-ymin)/2
23 N_0 = 60760
24 SWT_0 = math.sqrt(ymax*S_0)
25
26 S_90 = (ymax-ymin)/2
27 N_90 = 148339
28 SWT_90 = math.sqrt(ymax*S_90)
29
30 plt.loglog(N_0, SWT_0, 'r*', label='data-0')

```

```

31 plt.loglog(N_90, SWT_90, 'bx', label='data-90')
32
33 plt.xlabel('Number of cycles to failure')
34 plt.ylabel('$\sqrt{\sigma_{max}} \cdot \sigma_a$ [MPa]')
35 plt.legend()
36
37 plt.xticks([1E+4, 1E+5, 1E+6, 1E+7])
38 plt.yticks([100, 1000, 2000])
39
40 plt.savefig('swt_vs_cycles.png', dpi=300)
41
42 plt.show()

```

Listing A.11: Complete code for S-N diagram with SWT vs. number of cycles to failure as parameters.

```

1 import matplotlib.pyplot as plt
2 import numpy as np
3 import pandas as pd
4 import math
5
6 data_0 = pd.read_csv('data-0.csv', sep=";")
7 data_90 = pd.read_csv('data-90.csv', sep=";")
8
9 swt0NT = pd.read_csv('swt0NT.csv', sep=";")
10 swt0T = pd.read_csv('swt0T.csv', sep=";")
11 swt90NT = pd.read_csv('swt90NT.csv', sep=";")
12 swt90T = pd.read_csv('swt90T.csv', sep=";")
13
14 plt.figure(figsize=(5,5))
15
16 area = 6.5*3.25
17 stress_0 = (data_0.kN/area)*1000
18 stress_90 = (data_90.kN/area)*1000
19
20 ymax = 10000/(area)
21 ymin = 0/(area)
22
23 # Cycles for 0 and 90 specimen
24 x_xmax = data_0.cycles[np.argmax(data_0.cycles)]
25 x_xmax_90 = data_90.cycles[np.argmax(data_90.cycles)]
26
27 S_0 = (ymax-ymin)/2
28 N_0 = 60760

```

```

29 SWT_0 = math.sqrt(ymax*S_0)
30
31 S_90 = (ymax-ymin)/2
32 N_90 = 148339
33 SWT_90 = math.sqrt(ymax*S_90)
34
35 plt.loglog(N_0, SWT_0, 'r*', label='data-0')
36 plt.loglog(N_90, SWT_90, 'bx', label='data-90')
37
38 plt.loglog(swt0NT.X, swt0NT.Y, 'g^', label='90_NT')
39 plt.loglog(swt0T.X, swt0T.Y, 'yo', label='90_T')
40 plt.loglog(swt90NT.X, swt90NT.Y, 'ms', label='0_NT')
41 plt.loglog(swt90T.X, swt90T.Y, 'kD', label='0_T')
42
43 plt.xlabel('Number of cycles to failure')
44 plt.ylabel('$\sqrt{\sigma_{max}} \cdot \sigma_a$ [MPa]')
45 plt.legend()
46
47 plt.xticks([1E+4, 1E+5, 1E+6, 1E+7])
48 plt.yticks([100, 1000, 2000])
49
50 plt.savefig('swt_vs_cycles_merged.png', dpi=300)
51
52 plt.show()

```

Listing A.12: Complete code for comparing SWT vs. number of cycles to failure graph between this study and existing studies.

```

1 import cv2
2 import numpy as np
3
4 img = cv2.imread('Image_5652.tif', cv2.IMREAD_GRAYSCALE)
5 ret,thresh1 = cv2.threshold(img, 127, 255, cv2.THRESH_BINARY)
6 n_white_pix = np.sum(thresh1 == 255)
7 n_black_pix = np.sum(thresh1 == 0)
8 size = img.size
9 print('Number of white pixels:', n_white_pix)
10 print('Number of black pixels:', n_black_pix)
11 print('Total number of pixels in the image:', size)

```

Listing A.13: Complete code for measuring porosity.

```

1 import cv2
2 import numpy as np

```

```

3 import matplotlib.pyplot as plt
4
5 img = cv2.imread('Image_5652.tif',0)
6 ret,thresh1 = cv2.threshold(img, 127, 255, cv2.THRESH_BINARY)
7
8 titles = ['Original Image', 'Binary']
9 images = [img, thresh1]
10
11 for i in range(2):
12     plt.subplot(2,2,i+1), plt.imshow(images[i],'gray')
13     plt.title(titles[i])
14     plt.xticks([],plt.yticks([]))
15
16 plt.savefig('original_binary_porosity.png', dpi=300)
17
18 plt.show()

```

Listing A.14: Complete code for displaying the original porosity image vs. the binary image.

